



A Helicopter Simulator Assessment of Pilot Head Movement During Various Phases of Flight

By

**Malcolm G. Braithwaite
Eduardo A. Alvarez
Heber D. Jones
Alford A. Higdon
Shannon L. Groh**

Aircrew Health and Performance Division

and
Kathleen G. Beal

**Statistical Consulting Center
Wright State University**

and
Arthur Estrada

Hughes Technical Services

19970819 065

July 1997

DATA QUALITY ESTIMATED 4

Approved for public release, distribution unlimited.

**U.S. Army Aeromedical Research Laboratory
Fort Rucker, Alabama 36362-0577**

Notice

Qualified requesters

Qualified requesters may obtain copies from the Defense Technical Information Center (DTIC), Cameron Station, Alexandria, Virginia 22314. Orders will be expedited if placed through the librarian or other person designated to request documents from DTIC.

Change of address

Organizations receiving reports from the U.S. Army Aeromedical Research Laboratory on automatic mailing lists should confirm correct address when corresponding about laboratory reports.

Disposition

Destroy this document when it is no longer needed. Do not return it to the originator.


Disclaimer

The views, opinions, and/or findings contained in this report are those of the author(s) and should not be construed as an official Department of the Army position, policy, or decision, unless so designated by other official documentation. Citation of trade names in this report does not constitute an official Department of the Army endorsement or approval of the use of such commercial items.

Human use


Human subjects participated in these studies after giving their free and informed voluntary consent. Investigators adhered to AR 70-25 and USAMRMC Reg 70-25 on Use of Volunteers in Research.

Reviewed:




JEFFREY C. RABIN
LTC, MC
Director, Aircrew Health and Performance
Division

Released for publication:



JOHN A. CALDWELL, JR.
Chairman, Scientific
Review Committee


Dennis F. Shanahan, LTC, MFS
Colonel, MC, MFS
Commanding

Unclassified

SECURITY CLASSIFICATION OF THIS PAGE

REPORT DOCUMENTATION PAGE

Form Approved
OMB No. 0704-0188

1a. REPORT SECURITY CLASSIFICATION Unclassified			1b. RESTRICTIVE MARKINGS		
2a. SECURITY CLASSIFICATION AUTHORITY			3. DISTRIBUTION / AVAILABILITY OF REPORT Approved for public release, distribution unlimited		
2b. DECLASSIFICATION / DOWNGRADING SCHEDULE					
4. PERFORMING ORGANIZATION REPORT NUMBER(S) USAARL Report No. 97-26			5. MONITORING ORGANIZATION REPORT NUMBER(S)		
6a. NAME OF PERFORMING ORGANIZATION U.S. Army Aeromedical Research Laboratory		6b. OFFICE SYMBOL (If applicable) MCMR-UAD	7a. NAME OF MONITORING ORGANIZATION U.S. Army Medical Research and Materiel Command		
6c. ADDRESS (City, State, and ZIP Code) P.O. Box 620577 Fort Rucker, AL 36362-0577			7b. ADDRESS (City, State, and ZIP Code) Fort Detrick Frederick, MD 21702-5012		
8a. NAME OF FUNDING / SPONSORING ORGANIZATION		8b. OFFICE SYMBOL (If applicable)	9. PROCUREMENT INSTRUMENT IDENTIFICATION NUMBER		
8c. ADDRESS (City, State, and ZIP Code)			10. SOURCE OF FUNDING NUMBERS		
			PROGRAM ELEMENT NO.	PROJECT NO.	TASK NO.
			0602787A	3M162787A879	OA
11. TITLE (Include Security Classification) (U) A helicopter simulator assessment of pilot head movement during various phases of flight.					
12. PERSONAL AUTHOR(S) M.G. Braithwaite, E.A. Alvarez, A. Estrada, H.D. Jones, A.A. Higdon, S.L. Groh, & K.G. Beal					
13a. TYPE OF REPORT Final		13b. TIME COVERED FROM TO	14. DATE OF REPORT (Year, Month, Day) 1997 July		15. PAGE COUNT 51
16. SUPPLEMENTAL NOTATION					
17. COSATI CODES			18. SUBJECT TERMS (Continue on reverse if necessary and identify by block number)		
FIELD	GROUP	SUB-GROUP	Spatial disorientation, head movements, opto-kinetic & cervic reflex (OKCR).		
01	03	01			
19. ABSTRACT (Continue on reverse if necessary and identify by block number) The opto-kinetic cervico reflex (OKCR) is a recently hypothesized visually driven reflex that serves to stabilize the image of the external horizon on the retina during high performance aircraft roll maneuvers. Although anecdotally reported as occurring, head tilt during helicopter flight has not been formally studied. Such research is required to determine the full impact and significance it may have on a rotary-wing aviator's flying performance. The aim of this study was to investigate the relationship between horizon position and perception of orientation, and thus generate vital information to assess whether this reflex plays an important role in spatial disorientation. Twenty volunteer pilots participated in a UH-60 flight simulator study to examine the effects of this reflex. The results confirm that the OKCR occurs during simulated helicopter flight, both with and without night vision goggles. As with previous studies, head roll increased during flight under visual meteorological conditions in relation to increasing aircraft roll angle up to a maximum sustainable level and then remained constant. Head roll did not occur during flight under instrument meteorological conditions. Various aspects that impact rotary-wing operations are discussed, and recommendations made for future research.					
20. DISTRIBUTION / AVAILABILITY OF ABSTRACT <input checked="" type="checkbox"/> UNCLASSIFIED/UNLIMITED <input type="checkbox"/> SAME AS RPT. <input type="checkbox"/> DTIC USERS			21. ABSTRACT SECURITY CLASSIFICATION Unclassified		
22a. NAME OF RESPONSIBLE INDIVIDUAL Chief, Science Support Center			22b. TELEPHONE (Include Area Code) (334) 255-6907		22c. OFFICE SYMBOL MCMR-UAX-SI

Acknowledgments

The authors would like to acknowledge the willing assistance of the UH-60 simulator technicians: Richard Klein, Charles Brown, Robert Vandervelde, and Tom Schnormeier of Hughes Technical Services for keeping the simulator operational; James Lewis, Robert Dillard, and James Burkett for technical assistance; and Commander Fred Patterson, U.S. Navy and Captain Ron Merryman, U.S. Air Force, for providing comparative data from their own and other studies.

Table of contents

	<u>Page</u>
Introduction.....	1
Methods.....	3
Subjects.....	3
Apparatus.....	3
Flight profile.....	4
Task 1: NOE flight following a lead ship.....	4
Task 2: Contour altitude flight - independent slalom through pylons.....	4
Task 3: Contour altitude flight - figure 8.....	4
Task 4: IMC flight.....	5
Task 5: Contour altitude flight - coastline.....	5
Task 6: Unusual attitude recovery following loss of lead aircraft.....	5
Procedure.....	6
Statistical analysis.....	7
Results.....	8
Data distributions.....	8
ANOVA.....	8
Regression analysis.....	9
Day condition comparisons.....	10
Night condition comparisons.....	10
Comparison of day and night conditions.....	10
Comparison of motion and non-motion conditions.....	12
Comparison with other studies.....	14
Assessment of reversal error.....	15
Simulator sickness questionnaires.....	15
Discussion.....	17
Operational significance of the OKCR.....	19
Orientation during high angles of bank.....	19
Transition from VMC to IMC.....	19
HMDs.....	20
Future research.....	20
References.....	50
Appendix A Head tracker calibration data.....	A-1
Appendix B Summary of r-square values.....	B-1

Table of contents (continued)

List of tables	Page
1. Flight profile summary.....	7
2. Results of ANOVA for pilot head roll data	9
3. Summary of t-test results for comparison of day tasks	11
4. Summary of t-test results for comparison of night tasks.....	12
5. Summary of t-test results for comparison of day and night tasks	12
6. Summary of t-test and sign test results for comparison of motion/non-motion tasks.....	13
7. Summary of estimated slopes.....	14
8. Distribution of reversal error scores.....	15
9. Summary of t-test results for simulator sickness scores	16
B1. Summary of r-square values for day tasks	B-1
B2. Summary of r-square values for night tasks.....	B-2
B3. Summary of r-square values from day and night tasks.....	B-3
B4. Summary of r-square values from motion/nonmotion tasks.....	B-4

List of figures

1. G_z acceleration profile of task 1.....	21
2. G_z acceleration profile of task 2.....	21
3. G_z acceleration profile of task 3.....	22
4. G_z acceleration profile of task 4.....	22
5. G_z acceleration profile of task 5.....	23
6. G_z acceleration profile of task 6.....	23
7. Diagram of video camera setup.....	24
8. Still photograph from video recording.....	25
9. Ground track of task 1.....	26
10. Ground track of task 2.....	27
11. Ground track of task 3.....	28
12. Ground track of task 4.....	29
13. Ground track of task 5.....	30
14. Ground track of task 6.....	31
15. Scoring guide for reversal error.....	32
16. Histogram of task 1 (day) data sampling from all subjects for multiple levels of aircraft bank angle	33
17. Histogram of task 2 (day) data sampling from all subjects for multiple levels of aircraft bank angle	33

Table of contents (continued)

List of figures (continued)	<u>Page</u>
18. Histogram of task 3 (day) data sampling from all subjects for multiple levels of aircraft bank angle	34
19. Histogram of task 4 (day) data sampling from all subjects for multiple levels of aircraft bank angle	34
20. Histogram of task 5 (day) data sampling from all subjects for multiple levels of aircraft bank angle	35
21. Histogram of task 7 (day) data sampling from all subjects for multiple levels of aircraft bank angle	35
22. Histogram of task 6y (day) data sampling from all subjects for multiple levels of aircraft bank angle	36
23. Histogram of task 6z (day) data sampling from all subjects for multiple levels of aircraft bank angle	36
24. Histogram of task 1 (night) data sampling from all subjects for multiple levels of aircraft bank angle	37
25. Histogram of task 2 (night) data sampling from all subjects for multiple levels of aircraft bank angle	37
26. Histogram of task 3 (night) data sampling from all subjects for multiple levels of aircraft bank angle	38
27. Histogram of task 5 (night) data sampling from all subjects for multiple levels of aircraft bank angle	38
28. Histogram of task 7 (night) data sampling from all subjects for multiple levels of aircraft bank angle	39
29. Mean (± 1 SD) head roll as a function of aircraft bank angle. Task 1, day.....	40
30. Mean (± 1 SD) head roll as a function of aircraft bank angle. Task 2, day.....	40
31. Mean (± 1 SD) head roll as a function of aircraft bank angle. Task 3, day.....	41
32. Mean (± 1 SD) head roll as a function of aircraft bank angle. Task 4, day.....	41
33. Mean (± 1 SD) head roll as a function of aircraft bank angle. Task 5, day.....	42
34. Mean (± 1 SD) head roll as a function of aircraft bank angle. Task 7, day	42
35. Mean (± 1 SD) head roll as a function of aircraft bank angle. Task 6y, day	43
36. Mean (± 1 SD) head roll as a function of aircraft bank angle. Task 6z day.....	43
37. Mean (± 1 SD) head roll as a function of aircraft bank angle. Task 1, night.....	44
38. Mean (± 1 SD) head roll as a function of aircraft bank angle. Task 2, night.....	44
39. Mean (± 1 SD) head roll as a function of aircraft bank angle. Task 3, night.....	45
40. Mean (± 1 SD) head roll as a function of aircraft bank angle. Task 5, night.....	45
41. Mean (± 1 SD) head roll as a function of aircraft bank angle. Task 7, night.....	46
42. Mean head roll as a function of aircraft bank angle. Comparison with other studies.....	47
43. Mean head roll as a function of aircraft bank angle. Comparison of linear segments with other studies	47

Table of contents (continued)

	<u>Page</u>
List of figures (continued)	
44. Photograph of UH-60 simulator from the pilot's viewpoint	48
45. Photograph of UH-60 aircraft from the pilot's viewpoint	49

Introduction

An accurate perception of spatial orientation is fundamental to maintaining appropriate flight control. Spatial disorientation (SDO) is a major source of attrition, particularly in military flying. Recent reports (Braithwaite, 1994; Braithwaite et al., 1997b; Cheung et al., 1995; Durnford et al., 1995) have estimated that between 15 and 32 percent of severe aircraft accidents involved SDO. There is, therefore, a need to reduce mishaps by enhancing spatial awareness through improved training and display technology (Gillingham, 1992, Memorandum, 1996). Analysis of accident data suggests that although orientational cues may be present in the majority of mishaps, they are either not being interpreted correctly or do not receive the attention of the pilot. Both these phenomena may be attributed to limitations of cognitive processing.

There is a long held belief in much of the aeromedical literature that during flight, in conditions of good external visibility, pilots visually perceive a stabilized cockpit against an outside moving horizon (U.S. Navy, 1986; Dehart, 1985; Weintraub & Ensing, 1992; Sanders & McCormick, 1993; Gillingham & Previc, 1993). This assumed mechanism of visual orientation has driven the development of aircraft attitude displays. However, since many SDO related accidents are attributed to instrument misinterpretation, there is a continuing need for a better understanding of how pilots perceive and interpret spatial awareness.

In their work on resolving perceptual conflicts, Friederici and Levelt (1987) state there are three types of spatial orientation cues: retinal image coordinates, perceived coordinates of a viewed object or background, and gravitational sensations from the vestibular system. Since in-flight vestibular cues are known to be misleading, a pilot must depend on either retinal images or perceived object coordinates to maintain his spatial awareness. A stable retinal image serves as a point of reference for three-dimensional orientation or for tracking tasks requiring hand-eye coordination. In contrast, an unstabilized image moving across the retina causes a blurred low resolution retinal smear which is useful for detecting motion, but relatively ineffective in providing precise orientational cues (Brandt et al., 1972). Humans have evolved a number of higher reflexes to help stabilize retinal images during body movement in any of the three rotational axes (roll, pitch, and yaw). The vestibular-ocular reflex is one example of a physiological feedback loop that serves to coordinate eye movement for foveal image stabilization during rapid changes in head position. Additional examples of visual stabilization reflexes are the slow pursuit and rapid saccadic eye movements which function as a means to fix foveal images of moving targets.

Visually driven reflexes that emphasize stabilization of retinal images support the theory that pilots maintain head alignment with the horizon as a natural means of spatial orientation. By using a fixed horizon perspective, pilots can employ their sensory reflexes to stabilize the horizon image as a primary spatial cue, thereby improving the clarity of outside spatial cues. Simultaneously, relative cockpit motion can be detected from the peripheral field of view and thus provide pilots with important secondary spatial information. In contrast, if the pilot maintains head alignment with the cockpit, then horizon images will appear as low resolution

retinal smears during aircraft roll or pitch maneuvers, and so be much less effective at maintaining orientation.

Several recent studies (Patterson, 1995; Merryman and Cacioppo, 1997; Smith et al., 1997) have suggested that maintaining head alignment with a visually fixed image (such as the horizon) presents a more natural visual environment and therefore provides easier spatial interpretation. A behavior in the form of a reflex has been observed in high performance aircraft pilots in studies of both simulated and actual flight. It has been referred to as the opto-kinetic cervico reflex (OKCR). This visually-driven response causes a pilot to reflexively tilt his head toward the horizon during roll maneuvers. The response increases as aircraft roll angle is increased, up to a maximum head tilt, and then remains constant. This reflex is believed to improve spatial awareness by stabilizing the image of the real external horizon on the fovea in the manner described above. In contrast, in the absence of an outside horizon (such as during instrument flight), the visual stimulus provided by a head down cockpit instrument was discovered to be insufficient to cause reflexive head movement.

Although anecdotally reported as occurring, head tilt during helicopter flight has not been formally studied. Such research is required to determine the full impact and significance it may have on a rotary-wing aviator's flying performance. The aim of this study was to investigate the relationship between horizon position and perception of orientation, and thus generate vital information to assess whether this reflex plays an important role in SDO. In particular, it was anticipated that the findings would be important in resolving the debate over "roll-stabilization;" i.e., whether to stabilize the horizon symbol in a helmet mounted display (HMD) with the actual horizon, or enable it to move in the roll axis with relation to the pilot's head position.

To provide an appropriate corollary to Patterson (1995), Merryman and Cacioppo (1997), and Smith et al.'s (1997) work with high performance aircraft pilots, the objectives of this original research may be expanded as follows:

- To determine how helicopter pilots orient their heads when outside visual cues are present. The conditions examined for this objective were contour and nap of the earth (NOE) flight both in day visual meteorological conditions (VMC) and while wearing night vision goggles (NVGs). The primary emphasis was on the assessment of head roll.
- To evaluate pilot head orientation in flight environments that preclude outside visual cues in the transition to, and immersion in, simulated instrument meteorological conditions (IMC).
- To determine if SDO in the form of control reversal error could be induced following sudden transition to instruments during unusual attitude recovery.

Methods

Subjects

Twenty male military helicopter-rated pilots volunteered to participate in this study. Female pilots were not excluded but none volunteered. All subjects were in normal health and free of medication, and had not consumed excessive caffeine (> 5 cups of coffee or equivalent) or excessive alcohol (> 5 beers or equivalent) within the preceding 24 hours. Participants were asked to sign a volunteer agreement affidavit, and volunteer registry data sheets were maintained. These individuals were between the ages of 23 and 50 years, with a mean age of 35.6 years (standard deviation (SD) = 6.3). Total flight hours ranged from 146 to 8100 hours, with a mean of 2400 hours (SD = 1952).

Apparatus

The UH-60 simulator at the U.S. Army Aeromedical Research Laboratory (USAARL), Fort Rucker, Alabama, was used to examine the influence of the visually driven neck reflex described above on pilot orientation. Appropriate areas of the standard visual database and recordings of a simulated lead ship were chosen to stimulate the pilot to fly the simulator at aircraft roll angles between 0 and 80 degrees. The tasks are described in detail below. The simulator motion base was activated for all data runs of the main experiment.

Following the main experiment, four subjects repeated the flight profiles (less task 6) with the simulator motion based deactivated. Also, the acceleration environment of the flight tasks in the $\pm G_z$ direction was measured using an accelerometer attached to the floor beneath the pilot's seat. Although the simulator produces a negligible acceleration environment (see figures 1 through 6), the intention of this assessment was to determine whether the reflexive head movement was entirely visually driven. Comparisons of the "motion on" versus "motion off" data runs are reported in the results section of this report.

Measurement of head position in both sagittal and coronal planes (pitch and roll) was accomplished by using a Polhemus® 3 SPACE head tracker system. This system utilizes a low frequency magnetic field technology to determine the position and orientation of a sensor (receiver) in relationship to a source (transmitter). The angular resolution of this device is 0.0002 inches/inch of range, with a latency of 4.0 milliseconds from the center of the receiver measurement period to the beginning of transfer from the output port. The source unit was mounted in a fixed location approximately 40 inches vertical to the pilot's seat pan. The sensor unit was placed on top of the subject pilot's helmet during the simulated flight trials. During the flight profiles described below, pilot head orientation from the head tracker and aircraft parameter data were collected at a rate of 5 Hz using the simulator computer interface system. The head tracker has a boresight facility which allows calibration before each period of data collection. The accuracy of the head tracker was assessed at the beginning and end of the study and found to be satisfactory. The calibration results are recorded at appendix A.

Flight-serviceable aviator night vision imaging system (ANVIS) Mk6 NVGs were used during the night data runs.

Video recordings of each data collection run were performed using four cameras positioned as shown in figure 7. A strip of light emitting diodes was attached to the back of the pilot's helmet to aid observation of head roll in the low light conditions of the simulator cockpit. A composite four screen video picture was produced for each run. An example is shown in figure 8.

Flight profile

The flight profiles were designed to provide a distinctive set of visual conditions encountered in tactical flight, and for technical reasons, were in the same order on each flight.

Task 1: NOE flight following a lead ship

This task lasted approximately 7 minutes at an airspeed of 100-120 knots at 5-20 feet above ground level (AGL). The ground track is shown in figure 9. The objective of this task was to evaluate intermittent head roll in the coronal plane (plane perpendicular to the X axis) during transient aircraft banking maneuvers (low to moderate roll angle) with outside visual cues available. Data recording commenced at an airspeed of 15 knots following take-off and ended when the lead ship disappeared just prior to task 2. This task is referred to as DT1 for the day condition and NT1 for the night condition.

Task 2: Contour altitude flight - independent slalom through pylons

This was a timed task of exactly 3 minutes at an airspeed of 70-100 knots at 20-80 feet AGL. The ground track is shown in figure 10. The objective of this task was to evaluate head roll in the coronal plane during transient aircraft banking maneuvers (moderate to high roll angle) with outside visual cues. All turn points were clearly visible from the cockpit, and an investigator served as an "on board" navigator providing each pilot with verbal cues describing the direction and location of the next turn. Data recording commenced upon visual acquisition of the first pylon and ended after 180 seconds. This task is referred to as DT2 for the day condition and NT2 for the night condition.

Task 3: Contour altitude flight - figure 8

This task lasted approximately 4 minutes at an airspeed of 70-100 knots at 20-80 feet AGL. The ground track is shown in figure 11. The objective of this task was to evaluate head roll in the coronal plane during sustained aircraft banking maneuvers (moderate to high angle) with outside visual cues. Data recording commenced upon roll-in to the first loop of the figure 8 and ended when the second loop had been completed. This task is referred to as DT3 for the day condition and NT3 for the night condition.

Task 4: IMC flight

This task was conducted during day flight only. The ground track is shown in figure 12. The objective of this task was to evaluate head roll in the coronal plane during sustained aircraft banking maneuvers (low to moderate roll angle) without outside visual cues. It lasted approximately 8 minutes, and after a climb straight ahead from task 3 to 2000 ft AGL with a transition to IMC, the following maneuvers were performed at 120 knots:

- Expedite left turn to 90 degrees from track.
- Alter heading 10 degrees right.
- Alter heading 10 degrees left.
- Alter heading 30 degrees right.
- Alter heading 30 degrees left.
- Figure 8 turn at standard rate left, then right.
- Expedite right turn to 90 degrees from track.

Data recording commenced just prior to the first maneuver and ended when the pilot rolled out from the final maneuver. An IMC descent and breakout to VMC then followed to position the pilot for task 5. This task is referred to as DT4.

Task 5: Contour altitude flight - coastline

This task lasted approximately 6 minutes at an airspeed of 70-100 knots at 20-80 feet AGL. The ground track is shown in figure 13. The objective of this task was to evaluate head roll in the coronal plane during transient aircraft banking maneuvers (moderate to high angle) with outside visual cues. Data recording commenced upon coasting-in and ended once the island had been circumscribed. For the day data runs, the simulator was then reset to the runway for the start of task 6. This task is referred to as DT5 for the day condition and NT5 for the night condition.

Task 6: Unusual attitude recovery following loss of lead aircraft

This task was conducted during day flight only and lasted approximately 6 minutes at 70-120 knots airspeed at varying altitudes. The ground track is shown in figure 14. The objective of this task was twofold. First, the effect of attitude reference of a lone aircraft in poor visibility on head movement was evaluated, and second, the occurrence of reversal error once the lead ship had disappeared in IMC was assessed. Commencing with an initial value of 3.75 statute miles, external visibility was progressively decreased after 2 minutes at a step of 0.25 miles every 20 seconds down to 0.25 miles visibility. The external visual horizon became obscured at 2 miles visibility so that only the lead ship could be seen. The pilot's task was to follow the lead ship in line astern and execute the same roll and pitch maneuvers. Just prior to disappearing, the lead ship entered an attitude comprising approximately 15 degrees pitch up with a left roll angle of approximately 40 degrees. At this point, the subject was forced to

transition to instruments to overcome the unusual attitude, and then recover as directed by the simulator operator to the safety altitude, heading and airspeed. Control movements were observed and recorded. Data recording for this task were split into three discrete periods:

- a. From an airspeed of 15 knots following take-off until the external visual horizon was obscured (data referred to as task 6Y).
- b. From obscuration of the external visual horizon until the lead ship disappeared (data referred to as task 6Z).
- c. After the lead ship disappeared until the pilot had regained his safety altitude, airspeed and heading (data for this period was used to assess reversal error).

This was an unrealistic scenario for military rotary-wing pilots as standard operating procedures (SOPs) for inadvertent entry to IMC direct that aircraft flying in formation immediately deconflict in heading and altitude. Nevertheless, it could be accomplished safely in the simulator and the methodology enabled assessment of recovery from an unusual attitude induced by suddenly losing the only external visual cue. In order to maintain the "element of surprise," subjects were not trained on this task. Subjects were briefed that despite known SOPs, they were to maintain visual contact with the lead ship and follow its flight path, but if they lost sight of the lead ship, they should maintain or return to straight and level flight.

Procedure

Subjects were tested one at a time in the pilot's seat (right) of the USAARL UH-60 simulator. They wore flight suits and helmets. To avoid biasing the experiment, pilots were told that several physiological reflexes would be monitored in addition to control inputs and aircraft parameters. They were not advised prior to the experiment that head position was to be measured, or that a head tracker sensor would be attached to the top of their flight helmet.

The UH-60 simulator test flights lasted approximately 35 minutes as outlined above, and were preceded by a practice flight identical to both test flight conditions (although task 6 was omitted during training). Training included familiarization with the cockpit for non UH-60 rated pilots. The 2 conditions, day and half-moonlight (for NVG) were counterbalanced so that 10 subjects flew the NVG condition first and 10 subjects flew the day condition first. Subjects were randomly allocated to the two orders. A flight profile summary is shown in table 1.

Table 1.
Flight profile summary.

Task	Training (day)	Training (NVG)	Test (day)	Test (NVG)
1. NOE	√	√	√	√
2. Slalom	√	√	√	√
3. Figure 8	√	√	√	√
4. IMC	√	×	√	×
5. Island	√	√	√	√
6. UA recovery	×	×	√	×

√ = task performed

× = task not performed

As it is known (Gower and Fowkles, 1989) that flight in the UH-60 simulator may provoke simulator sickness syndrome (SSS), all subjects were closely monitored and questionnaires designed by Lane and Kennedy (1988) were administered before and after each test flight.

Statistical analysis

The raw data comprised head roll angle and the simulator roll angle. Right aircraft and head roll was regarded as positive, and left roll negative. The data samples were compiled into subject files corresponding to the appropriate task (1 through 6Z). A composite data file (task 7, referred to as DT7 for the day condition and NT7 for the night condition) comprising data from all the VMC tasks (1, 2, 3, and 5) was also made. Each record in the file contained a single time annotation with corresponding samples of aircraft attitude and head angle. Samples of aircraft roll were then used to sequentially arrange the records in each file. Records were then further subdivided into 32 5-degree increments of aircraft bank labeled -80 degrees through zero to +75 degrees (the cell label represents the lowest value in the cell). Individual data files were stored in ASCII format and then analyzed using STATISTICA® statistical software and SAS for Windows Version 6.11®. Corresponding head tracker values for each increment were then averaged.

The factorial design for the analysis of variance (ANOVA) of tasks 1 through 6Z consisted of one dependent variable (head roll angle) compared against multiple levels of a single independent measure (aircraft roll angle). Linear regression techniques were then used to compare the data curves of aircraft roll angle against head roll angle (in 5 degree increments).

In order to assess the occurrence of reversal error upon initial recovery from the unusual attitude at the end of task 6, the direction of initial cyclic stick movement (over the first 5 seconds) was recorded in the manner described by Braithwaite et al., 1997a. The ideal initial direction of cyclic movement to restore the aircraft attitude to wings level and then pitch level was calculated. A score was then awarded according to the actual direction of cyclic movement. The initial cyclic movement should be to the right followed by a forward movement as shown in figure 15. A maximum score of 4 was awarded if this was the case. Initial movements in other directions were awarded the number of points illustrated in the quadrant; e.g., an initial left movement of the cyclic would score 0, and a downward right movement would score 2.5. The scores were then subjected to ANOVA against appropriate independent variables.

Results

Data distributions

As there was no control over specific angles of bank during aircraft turns, the subjects employed each of the 32 levels of aircraft roll angle differently, and so some cells did not contain data. Figures 16 through 28 are histograms illustrating the distribution of aircraft roll data for each task.

ANOVA

Dependent variable data that were not normally distributed were transformed to \log_e values prior to analysis. Prior to analysis, missing data were replaced by the means of the remaining cell data values with the following exception. If the independent variables of aircraft roll contained data from three or less subjects, these values were discarded. Had this not been done, the variance would have been unrepresentative for that dependent variable. The results of ANOVA are summarized in table 2. Aircraft roll had a highly significant effect on head roll in all tasks except task 4 (IMC flight).

Table 2.
Results of ANOVA for pilot head roll data.

Task	variables (degree cells)	No. of levels of variable	df	df error	MS error	F	p-value
Day 1	-60 to +40	21	20	380	11.82	334.33	<0.001
Day 2	-75 to +65	29	28	532	22.35	335.16	<0.001
Day 3	-55 to +40	20	19	361	21.41	200.08	<0.001
Day 4	-25 to +25	11	10	190	0.07	1.07	0.386
Day 5	-80 to +70	31	30	570	19.88	322.09	<0.001
Day 6Y	-40 to +20	13	12	228	10.36	120.46	<0.001
Day 6Z	-55 to +45	21	20	380	6.48	69.56	<0.001
Day 7	-80 to +70	31	30	570	19.81	345.56	<0.001
Night 1	-60 to +35	20	19	361	9.55	325.06	<0.001
Night 2	-70 to +60	27	26	494	17.47	420.80	<0.001
Night 3	-55 to +45	21	20	380	16.20	234.02	<0.001
Night 5	-80 to +70	31	30	570	13.38	433.90	<0.001
Night 7	-80 to +70	31	30	570	13.78	456.53	<0.001

shaded cells are nonsignificant

Regression analysis

Figures 29 through 41 are plots of aircraft roll for all tasks against the means ± 1 SD for all subjects .

Regression analysis was conducted in four ways: day condition comparisons, night condition comparisons, day/night condition comparisons, and motion/non-motion comparisons. The analysis for each set of comparisons is similar. A simple linear regression model was fitted for each subject/task combination. In order to compare two tasks, the estimates of the slope for a given subject and pair of tasks were subtracted, and then a paired t-test was run on the set of differences. If the mean difference was statistically different from zero, it may be concluded that the relationship between head roll and horizontal roll is not the same for the two tasks. The results of the paired t-tests are illustrated in tables 3 through 6 in this section, while the tables for r-squares values for the regressions are at appendix B.

Day condition comparisons

Table B-1 summarizes the r-square values from each regression. The r-square values are consistently high for all tasks except four. For task DT4, the values were quite variable. Two other values of r-square stood out. For task DT6Y, subject eight had a lower r-square than his counterparts. Also, for task DT6Z, subject six had a lower r-square value than the others.

Table 3 summarizes the results of the paired t-tests. Since 19 tests were performed, the overall type I error rate was protected by using the sequential Bonferroni method. This involves dividing the overall α (0.05) by the number of tests. In this case, the significance for the test with the smallest p-value is decided on a level of significance of $0.05/21 = 0.0024$. The second smallest p-value is considered significant if less than $0.05/20$, etc. By this criterion, all compared tasks differed except 1 vs. 2, 1 vs. 3, 1 vs. 5, 1 vs. 6Y, 2 vs. 3, and 5 vs. 6Y. For all other task comparisons, there is statistical evidence that the relationship between head roll and horizontal roll differs for the compared tasks. In the cases where the t-statistics and mean difference are negative, the slope for the task with the lower number tends to be negative and steeper than the task with the higher value. For the higher numbered task of the pair, the slopes are close to zero, some positive and some negative. In the instances where the t-statistic and mean difference are positive, the relationship is reversed. That is, the slopes for the higher numbered task tend to be negative and steeper than those for the lower numbered task. The comparison of tasks 1 and 6Y is only marginally significant.

Night condition comparisons

Table B-2 summarizes the r-square values from each regression. The r-square values are high for all subjects in all tasks. Table 4 summarizes the results of the paired t-tests. Again, the overall type I error rate was protected for these six tests by using the sequential Bonferroni method as described above. In this case, the significance for the test with the smallest p-value is decided on a level of significance of $0.05/6 = 0.0083$. The second smallest p-value is considered significant if less than $0.05/5$, etc. By this criterion, there are significant differences between tasks 1 vs. 2, 2 vs. 5, and 3 vs. 5. For tasks 1 and 2, the slopes are all negative. Those for task 2 tend to be steeper than those for task 1. The slopes of tasks 2, 3, and 5 are also all negative. The slopes of tasks 2 and 3 tend to be steeper than those of task 5.

Comparison of day and night conditions

Table B-3 summarizes the r-square values from each regression for the tasks that were replicated in both day and night conditions (tasks 1, 2, 3, 5, and 7). Many of the r-square values are repeats from earlier tables. Only those for DT7 and NT7 are new. The r-square values are all high.

Day and night task pairs were compared: DT1 to NT1, DT2 to NT2, DT3 to NT3, DT5 to NT5, and DT7 to NT7. Table 5 summarizes the results. As before, the overall type I error rate

was controlled using the sequential Bonferroni method. There were no strong significant differences in the slopes of the tasks. There was a marginal significance for the comparison of DT1 and NT1. All slopes were negative, those for DT1 tending to be steeper than those for NT1.

Table 3.
Summary of t-test results for comparison of day tasks.

Tasks compared	t-statistic	df	p-value	Mean \pm SD
1, 2 (DT1, DT2)	1.58	19	0.1296	0.033 \pm 0.094
1, 3 (DT1, DT3)	2.04	19	0.0559	0.044 \pm 0.097
1, 4 (DT1, DT4)	-19.51	19	0.0001	-0.458 \pm 0.105
1, 5 (DT1, DT5)	-1.82	19	0.0849	-0.024 \pm 0.060
1, 6Y (DT1, DT6Y)	-2.35	19	0.0297	-0.057 \pm 0.109
1, 6Z (DT1, DT6Z)	-18.10	19	0.0001	-0.267 \pm 0.066
2, 3 (DT2, DT3)	0.38	19	0.7067	0.011 \pm 0.127
2, 4 (DT2, DT4)	-17.06	19	0.0001	-0.492 \pm 0.129
2, 5 (DT2, DT5)	-3.39	19	0.0031	-0.058 \pm 0.076
2, 6Y (DT2, DT6Y)	-3.82	19	0.0012	-0.091 \pm 0.106
2, 6Z (DT2, DT6Z)	-14.31	19	0.0001	-0.300 \pm 0.094
3, 4 (DT3, DT4)	-15.26	19	0.0001	-0.503 \pm 0.147
3, 5 (DT3, DT5)	-3.18	19	0.0050	-0.069 \pm 0.096
3, 6Y (DT3, DT6Y)	-3.53	19	0.0022	-0.101 \pm 0.129
3, 6Z (DT3, DT6Z)	-12.80	19	0.0001	-0.311 \pm 0.109
4, 5 (DT4, DT5)	17.74	19	0.0001	0.434 \pm 0.109
4, 6Y (DT4, DT6Y)	10.55	19	0.0001	0.401 \pm 0.170
4, 6Z (DT4, DT6Z)	10.40	19	0.0001	0.191 \pm 0.082
5, 6Y (DT5, DT6Y)	-1.26	19	0.2239	-0.033 \pm 0.117
5, 6Z (DT5, DT6Z)	-15.13	19	0.0001	-0.243 \pm 0.072
6Y, 6Z (DT6Y, DT6Z)	-7.93	19	0.0001	-0.210 \pm 0.118

shaded cells are nonsignificant

Table 4.
Summary of t-test results for comparison of night tasks.

Tasks compared	t-statistic	df	p-value	Mean \pm SD
1, 2 (NT1, NT2)	4.62	19	0.0002	0.075 \pm 0.073
1, 3 (NT1, NT3)	2.14	19	0.0453	0.046 \pm 0.096
1, 5 (NT1, NT5)	-1.28	19	0.2148	-0.018 \pm 0.063
2, 3 (NT2, NT3)	-1.32	19	0.2020	-0.029 \pm 0.099
2, 5 (NT2, NT5)	-6.37	19	0.0001	-0.093 \pm 0.066
3, 5 (NT3, NT5)	-3.73	19	0.0014	-0.064 \pm 0.077

shaded cells are nonsignificant

Table 5.
Summary of t-test results for comparison of day and night tasks.

Tasks compared	t-statistic	df	p-value	Mean \pm SD
Task 1. Day / night DT1, NT1	-2.40	19	0.0271	-0.033 \pm 0.061
Task 2. Day / night DT2, NT2	0.70	19	0.4902	0.009 \pm 0.059
Task 3. Day / night DT3, NT3	-1.43	19	0.1675	-0.031 \pm 0.096
Task 5. Day / night DT5, NT5	-2.08	19	0.0514	-0.026 \pm 0.057
Task 7. Day / night DT7, NT7	-1.80	19	0.0885	-0.020 \pm 0.049

shaded cells are nonsignificant

Comparison of motion and non-motion conditions

Table B-4 summarizes the r-square values from each regression. The r-square values are high but for four exceptions (subjects 5, 10, and 14 for DT4 [motion on], and subject 10 for DT4 [motion off]). Table 6 summarizes the results of the paired t-tests. Because the sample size was small, the results of the nonparametric sign test are also included. As before, the overall type I error rate for the six tests for the day data was controlled using the sequential Bonferroni method.

In this case, the significance for the test with the smallest p-value is decided on a level of significance of $0.05/6 = 0.0083$. Since the smallest p-value is 0.0175, it was concluded that the average difference in slopes for the two conditions was not significantly different from zero. The sign test results are consistent with this conclusion. Since five tests were performed for the night data, the significance for the test with the smallest p-value is decided on a level of significance of $0.05/5 = 0.010$. Two results were less than this value and it was concluded that the difference between the slopes is statistically different from zero. All the slopes are negative. In the case of comparing NT5 (motion on) to NT5 (motion off), the slopes for the first task are steeper than those for the second. Likewise, the slopes of NT7 (motion on) and NT7 (motion off) are also negative. Those for NT7 (motion on) are steeper than those for NT7 (motion off). However, the results of the sign test do not corroborate these results.

Table 6.

Summary of t-test and sign test results for comparison of motion/non-motion tasks.

Tasks compared	t-statistic	df	p-value	Mean \pm SD	Sign statistic	p-value
Day task 1	-0.08	3	0.9439	-0.002 \pm 0.050	1	0.6250
Day task 2	-4.77	3	0.0175	-0.092 \pm 0.039	-2	0.1250
Day task 3	-0.83	3	0.4670	-0.022 \pm 0.054	-1	0.6250
Day task 4	-0.29	3	0.7921	-0.003 \pm 0.023	-1	0.6250
Day task 5	-3.15	3	0.0513	-0.078 \pm 0.049	-2	0.1250
Day task 7	-2.41	3	0.0949	-0.063 \pm 0.052	-1	0.6250
Night task 1	-0.59	3	0.5990	-0.022 \pm 0.075	-1	0.6250
Night task 2	-1.30	3	0.2840	-0.032 \pm 0.050	-1	0.6250
Night task 3	0.53	3	0.6315	0.010 \pm 0.040	0	0.1000
Night task 5	-9.88	3	0.0022	-0.080 \pm 0.016	-2	0.1250
Night task 7	-6.39	3	0.0077	-0.070 \pm 0.022	-2	0.1250

shaded cells are nonsignificant

Comparison with other studies

Three sets of data from two previous studies of the OKCR (Merryman and Cacioppo, 1997 and Smith et al., 1997) were made available so that the composite VMC data for the day condition of this study could be compared. This is illustrated in figure 42.

A regression analysis of the linear segment (from -30 degrees to +30 degrees of aircraft bank) was performed. The four data sets are illustrated in figure 43, and table 7 summarizes the estimated slopes.

Table 7.
Summary of estimated slopes.

Study	ESTIMATED SLOPE
Merryman and Cacioppo	-0.291754
Smith et al. (active)	-0.330840
Smith et al., (passive)	-0.452380
Braithwaite et al	-0.564233

In order to determine whether the slope from this study differed significantly from the other three data sets, a 95 percent confidence interval was created using the following formula:

estimated slope $\pm t_{\alpha/2}$ standard error.

$$= -0.564233 \pm t_{0.05/2} (0.01390737)$$

$$= -0.564233 \pm 2.201 (0.01390737)$$

$$\therefore 95 \text{ percent confidence interval} = (-0.5948429, -0.533623)$$

This interval does not contain the estimates of the slopes from the previous studies. It is therefore concluded that the slope from this study differs from the other three.

Assessment of reversal error

The occurrence of reversal error was assessed during recovery from the unusual attitude at the end of task 6. Initial cyclic stick movements were recorded and analyzed as described above. Table 8 shows the distribution of scores. By these criteria, five subjects (25 percent of the pool) showed definite reversal error (scores of 1.0 or less). ANOVA revealed that there was no significant difference in these scores between the independent variables of years flown, flying hours or type of current aircraft flown.

Table 8.
Distribution of reversal error scores.

Reversal error score	Number of subjects
0.0	0
0.5	0
1.0	5
1.5	0
2.0	3
2.5	6
3.0	0
3.5	0
4.0	6

Simulator sickness questionnaires

Pre- and postflight SSS scores for the two flight conditions (day and night) were analyzed using paired t-tests for dependent samples. The results are summarized in table 9. The only significant results were for the total score for the day condition, and nausea scores for the night condition. However, these were only marginally significant, and the scores were not of significant magnitude to suggest that simulator sickness was a serious problem.

Table 9.
Summary of t-test results for simulator sickness scores.

Simulator sickness parameter	Day/night	Pre/post flight	t-statistic	df	p-value	Mean \pm SD
Nausea	Day	Pre	-1.93	19	0.069	103.3 \pm 7.1
Nausea	Day	Post				108.6 \pm 12.3
Visual	Day	Pre	-1.36	19	0.189	104.5 \pm 7.1
Visual	Day	Post				107.6 \pm 9.2
Disorientation	Day	Pre	-2.01	19	0.059	102.1 \pm 9.3
Disorientation	Day	Post				111.8 \pm 22.7
Total	Day	Pre	-2.12	19	0.048	104.3 \pm 6.7
Total	Day	Post				110.5 \pm 12.4
Nausea	Night	Pre	-2.28	19	0.034	103.3 \pm 7.1
Nausea	Night	Post				107.7 \pm 10.1
Visual	Night	Pre	-0.44	19	0.666	104.9 \pm 6.6
Visual	Night	Post				105.7 \pm 5.4
Disorientation	Night	Pre	-1.63	19	0.119	100.7 \pm 3.1
Disorientation	Night	Post				106.3 \pm 15.3
Total	Night	Pre	-1.91	19	0.072	103.9 \pm 4.9
Total	Night	Post				107.5 \pm 8.8

shaded cells are nonsignificant

Discussion

When Patterson (1995) first described the OKCR, he concluded that this involuntary neck response appeared to be generated by motion of retinal images as opposed to a vestibular stimulus. Its purpose is thought to be to stabilize the external horizon as a primary spatial reference that extends through the fovea and across the peripheral field of view. Peripherally viewed images such as cockpit structures and, in the case of helicopter flight, the path of the main rotor disc, function as secondary spatial cues that provide rate and position change relative to the visually stabilized horizon. Patterson also states that the benefit in establishing this spatial perspective is that visual feedback from the peripherally viewed images will move in a direction compatible with joystick (or cyclic) control inputs. Other sensory reflexes exist to enhance orientation. These reflexes include the vestibulo-ocular reflex, optokinetic nystagmus, and ocular torsion. The OKCR is the most recently described of these complex physiological phenomena whose contribution to man's orientation in an unfamiliar environment has only recently been recognized.

The results of this study confirm that the OKCR occurs during simulated helicopter flight, both with and without NVGs. As with previous studies, head roll increased in relation to increasing aircraft roll angle up to a maximum sustainable level and then remained constant. Various aspects are discussed below.

In the day condition phase of this study, aircraft roll had a consistent and highly significant effect on head roll in all tasks except task 4 (IMC flight). In this latter case, Patterson's findings (1995) are replicated in that the symbology motion from the standard "moving horizon" attitude direction indicator appears to be insufficient to trigger a measurable OKCR response. Regression analysis of this task against all others confirmed a significant difference in the slopes. It is of special interest that even in flight conditions of poor visibility where the only external attitude reference is a lead aircraft (task 6Z), the OKCR was still elicited, albeit to a lesser degree. This finding confirms the generator of the response as being external images viewed against a peripheral background of cockpit structures. Furthermore, as seen in previous studies (Patterson, 1995; Smith et al., 1997) the OKCR was elicited in this helicopter simulator both with the motion base on and off. There was no significant difference between the "motion on" and "motion off" data in this study and, especially as the G_z environment of the "motion on" runs was consistently low ($1g \pm 0.03g$), the purely visual nature of the reflex is supported.

In the night condition phase during flight with NVGs, aircraft roll continued to have a highly significant effect on head roll. Prior to the study it had been expected that head roll would be limited during the NVG assessment because of the increased head-mounted mass and altered center of gravity. However, analyses comparing day and NVG flight showed no strong significant differences in the magnitude of the OKCR between the two conditions. This provides further evidence of the fundamental nature of the OKCR and that it does not appear to be affected by a restricted field of view.

It can be seen in all of the VMC task curves that head roll initially increases linearly in an opposite direction to aircraft roll (\pm c. 30 degrees) and then levels off, or even decreases. As suggested by Patterson (1995) and endorsed by Merryman and Cacioppo (1997), during these low angles the pilot maintains an almost fixed visual orientation with respect to the horizon - the aircraft and pilot's body moving independently from his head. However, at higher angles of bank (>30 degrees), the OKCR response levels and the pilot's head begins to move with the aircraft and against the horizon image. This reflects a significant transition in visual orientation cues and reference frame. In this study the asymptotic limit of pilots' head roll was in the range of 15 to 25 degrees of lateral flexion (depending on the task), and was similar in value to data from the high performance aircraft studies. This limit is much less than the recorded mean male anthropometric limit of lateral flexion of 41 degrees (Woodson et al., 1992). Merryman and Cacioppo (1997) suggest that this observed limitation may either be a function of comfort, or due to a cognitive recognition that at higher angles of bank, the rotated horizon is no longer a familiar pattern, and thus ceases to be a primary visual cue to maintain spatial orientation. Further work is required to identify the contribution of these two processes to the OKCR.

This study was intended as a sequel to previous work. It is therefore appropriate to directly compare the results with previous studies that have assessed the OKCR. Patterson's (1995) subject flew a simulated F-15 mission in a static dome simulator. Smith et al.'s study (1997) used similar apparatus, again during F-15 missions, but included both an "active" phase, in which the subjects controlled the simulator, and a "passive" phase during which the autopilot flew the mission while the subject acted as the navigator. Merryman and Cacioppo measured head roll during actual training flights in the F-15. Their work comparing the linear segments of the OKCR response suggests that there was not a significant difference between Smith et al.'s "active" simulator condition and their own in-flight data. They concluded that these results validated simulator research as a means to study the OKCR. While comparison of the aircraft vs. head roll curve of this study with others (figure 42) shows a similar trend in the OKCR response, the 95 percent confidence interval of the estimate of the slope of the linear portion of the curve does not contain the estimates of the slopes from the previous studies. It therefore appears unexpectedly that head roll of subject pilots in this helicopter simulator study was significantly greater than in the high performance aircraft studies. A possible reason for this finding is the restriction of forward visibility in the UH-60 simulator compared to the real aircraft. Figures 44 and 45 illustrate the differences in external visibility from the pilot's viewpoint. Furthermore, the videotapes suggested that subjects combined upper body roll with head roll during some of the extreme roll maneuvers. Assessment of the OKCR during actual flight would help to resolve this apparent discrepancy.

Nine of the 14 subjects in Patterson's study (1995) exhibited reversal error during recovery from an unusual attitude, whereas only five subjects in this study were assessed as committing definite reversal error. The reasons for this are possibly twofold. First, there was a difference in the measurement of reversal error between the two studies; and second, the final attitude of the

helicopter just prior to recovery was not as severe as that of the F-15. Nevertheless, the incidence of reversal error in this study (25 percent), confirms that the occurrence of SDO generated in this way may be a significant problem.

Operational significance of the OKCR

The results of this and previous research confirm the suggestion by Smith et al., (1997) that the historical assumption that a pilot maintains head alignment with the body axis during roll maneuvers must be refuted. The existence of the OKCR must therefore be considered during the analysis of pilots' spatial orientation during high angles of bank, during the transition from VMC to IMC, and in the design of aircraft attitude instruments. The latter is of particular importance for HMDs. Each is discussed below.

Orientation during high angles of bank

The operational extremes of helicopter bank angle (up to 60 degrees) were exceeded in this simulator study so that the full spectrum of OKCR response could be studied. Tasks 2 and 5 were the most demanding in that high aircraft bank angles were necessary to negotiate the planned ground track. It was only during these tasks that simulator crashes occurred which were always associated with high bank angles. This finding lends credence to the theory that spatial orientation at extreme bank angles may be impaired as discussed above. However, unlike high performance aircraft, helicopters rarely exceed these limits for more than a few seconds. Indeed, as the majority of military helicopter operations take place close to the ground, aviators are unlikely to exceed 45 degrees angle of bank except during aerial combat maneuvers. Therefore, it may be possible that helicopter pilots are less "affected" by the OKCR than their high performance aircraft counterparts. This aspect can only be satisfactorily studied during actual flight within the operational flight parameters for the appropriate altitude.

Transition from VMC to IMC

Both this and a previous helicopter simulator study (Braithwaite et al., 1997a) have demonstrated the occurrence of reversal error during recovery from unusual attitudes and transition from VMC to IMC. Theoretically, the OKCR probably contributes to the misinterpretation of instrument attitude information during this transition, but its actual contribution to helicopter incidents and accidents is unknown. The consequences of the traditional design of aircraft instruments that have "ignored" the OKCR may have been a feature in some SDO related mishaps in high performance aircraft. However, there is no substantiated evidence that rotary-wing accidents have occurred as a result. Now that this physiological behavior has been brought to light, accident investigators should consider the phenomenon during mishaps in which SDO is suspected.

HMDs

Both Patterson (1995) and Merryman and Cacioppo (1997) stress the importance of considering the existence of the OKCR in the design and application of HMDs. The main concern is that HMDs have a frame of reference that is primarily based on the pilot's head. The pilot's head is subject to the OKCR response which changes the pilot's cognitive frame of reference during flight. Hypothetically, therefore, the displayed attitude reference should be "roll stabilized" with respect to the pilot's head position. However, one of the fundamental purposes of HMDs is to provide orientation and targeting information when the pilot is not looking forward (off axis). There is anecdotal evidence (McLean, 1997) that although it is theoretically more satisfactory, helicopter pilots who have flown with experimental HMDs in which the horizon symbology was stabilized, do not like the concept. They found it to be disorienting when looking off bore sight. This may either be a function of previously learned experience or of poor HMD symbology design, and is worthy of further research.

Future research

From the discussion above, it is clear that much more needs to be determined about the effect of this recently defined phenomenon. These may be summarized as follows:

- The OKCR should be studied in actual helicopter flight.
- The relationship between the OKCR and ocular torsion should be investigated.
- The "comfortable" anthropometric limits of lateral head flexion should be investigated.
- The effect of the existing NVG head up display on the OKCR should be investigated.

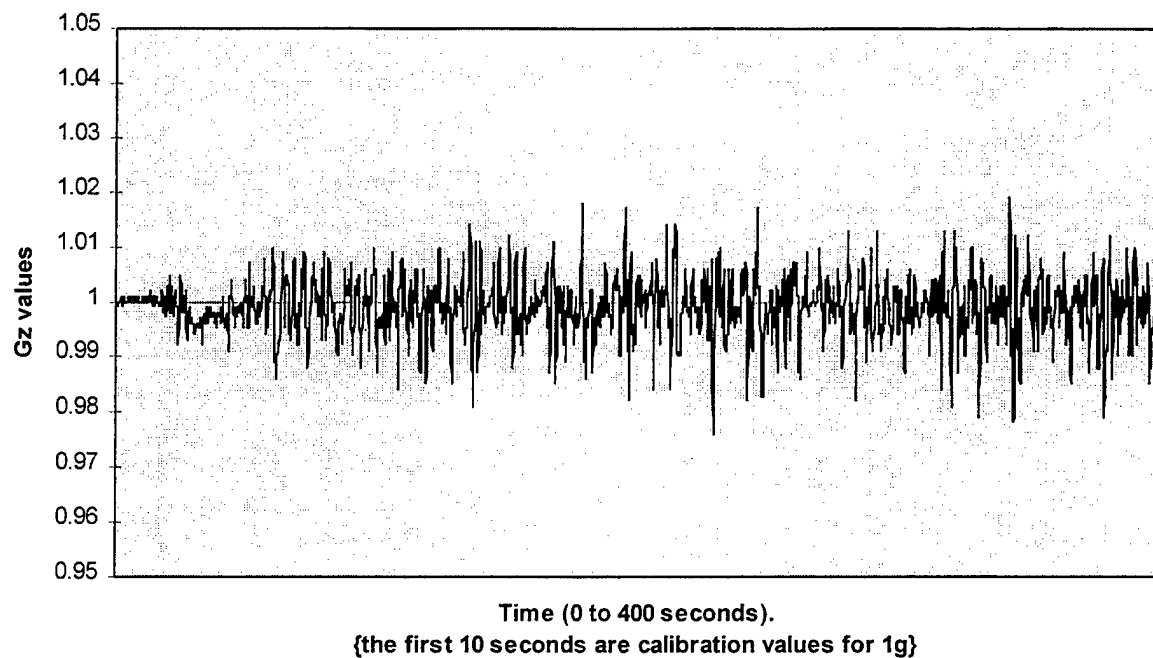


Figure 1. G_z acceleration profile of task 1.

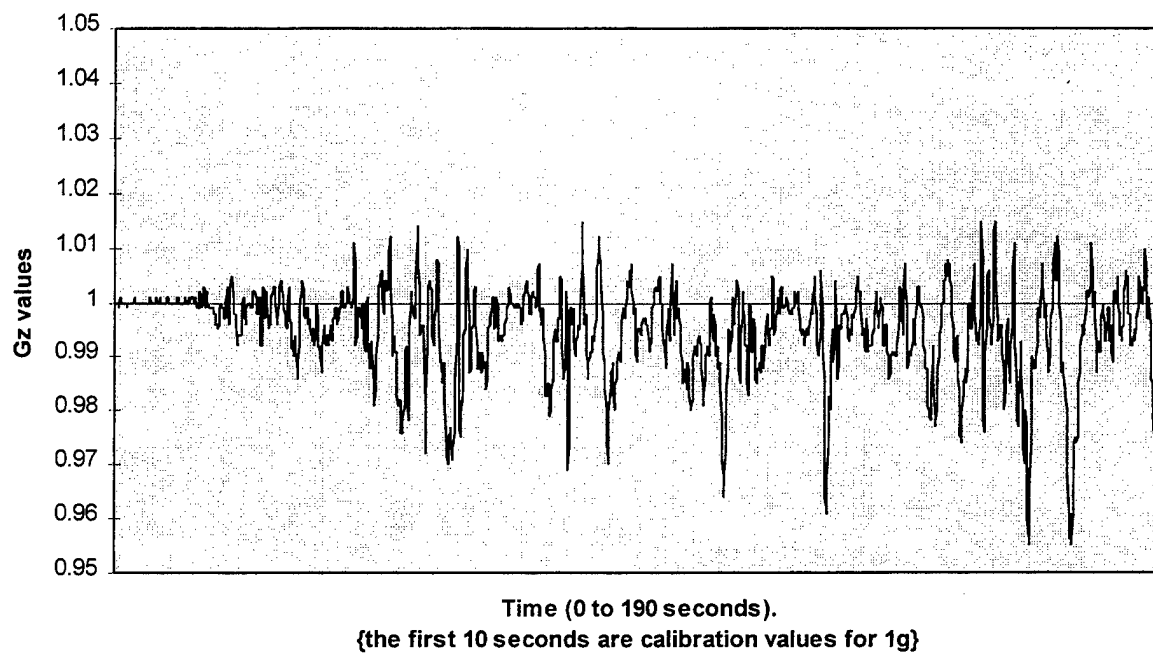


Figure 2. G_z acceleration profile of task 2.

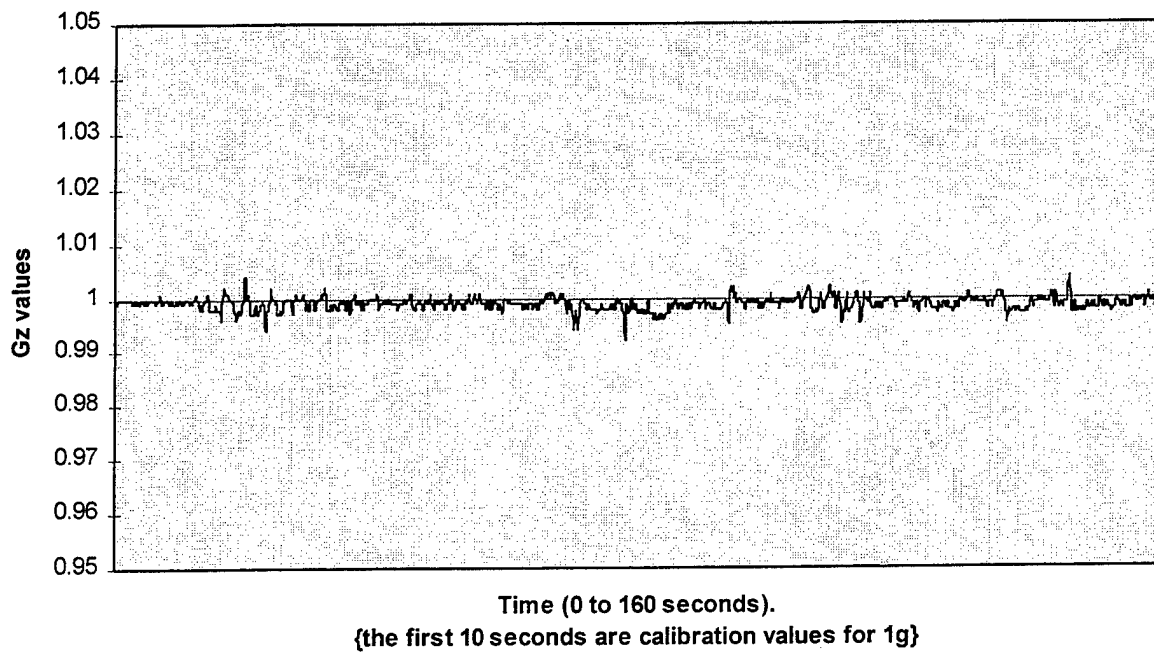


Figure 3. G_z acceleration profile of task 3.

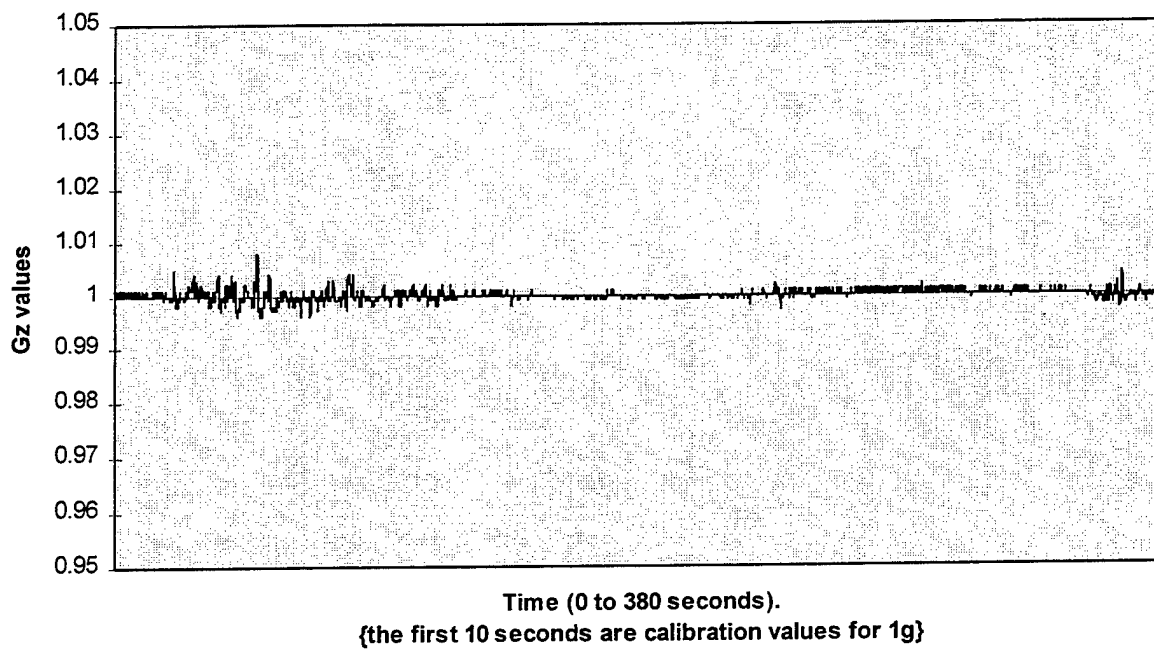


Figure 4. G_z acceleration profile of task 4.

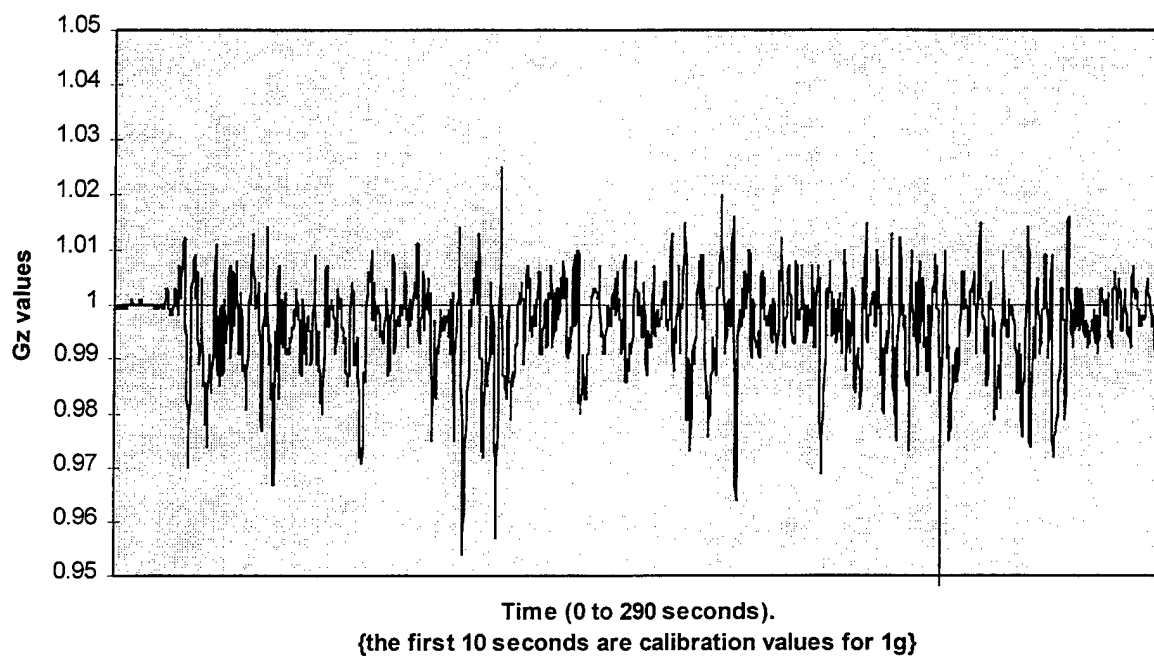


Figure 5. G_z acceleration profile of task 5.

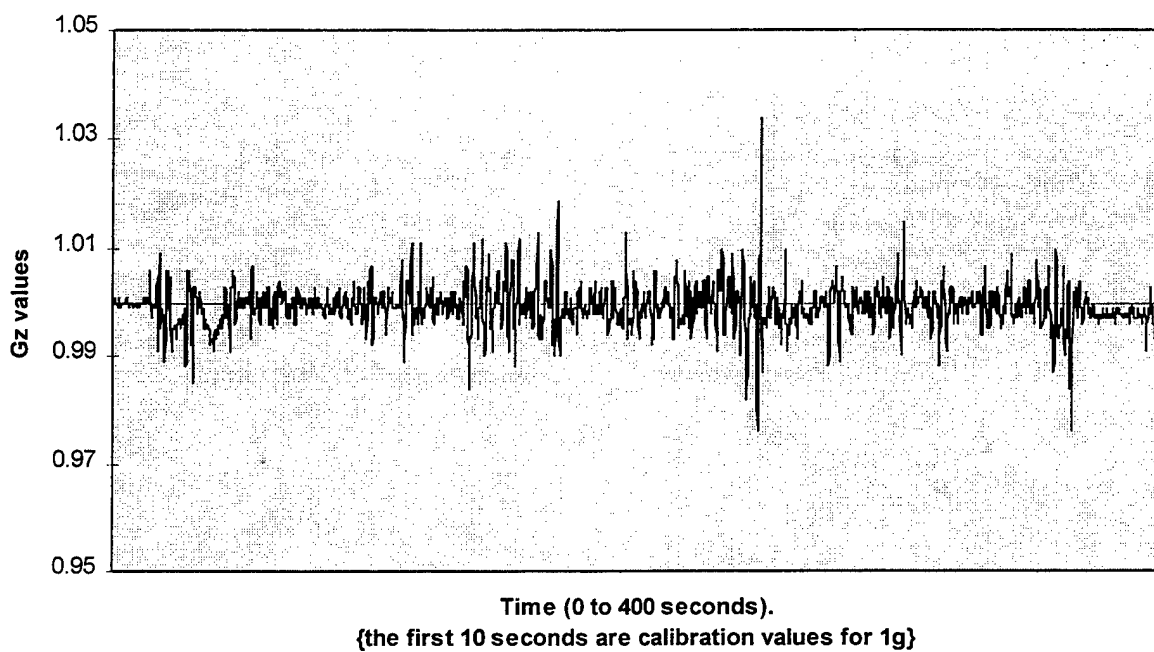


Figure 6. G_z acceleration profile of task 6.

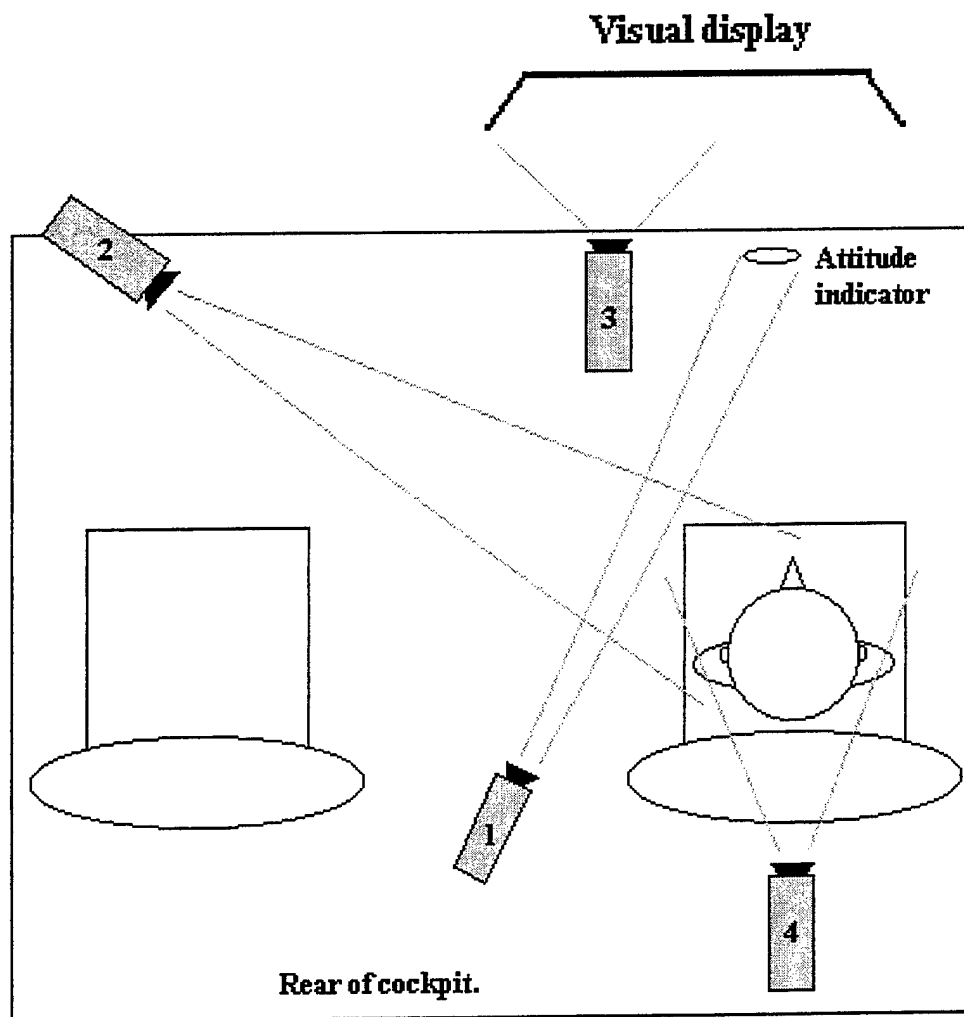


Figure 7. Diagram of video camera setup.

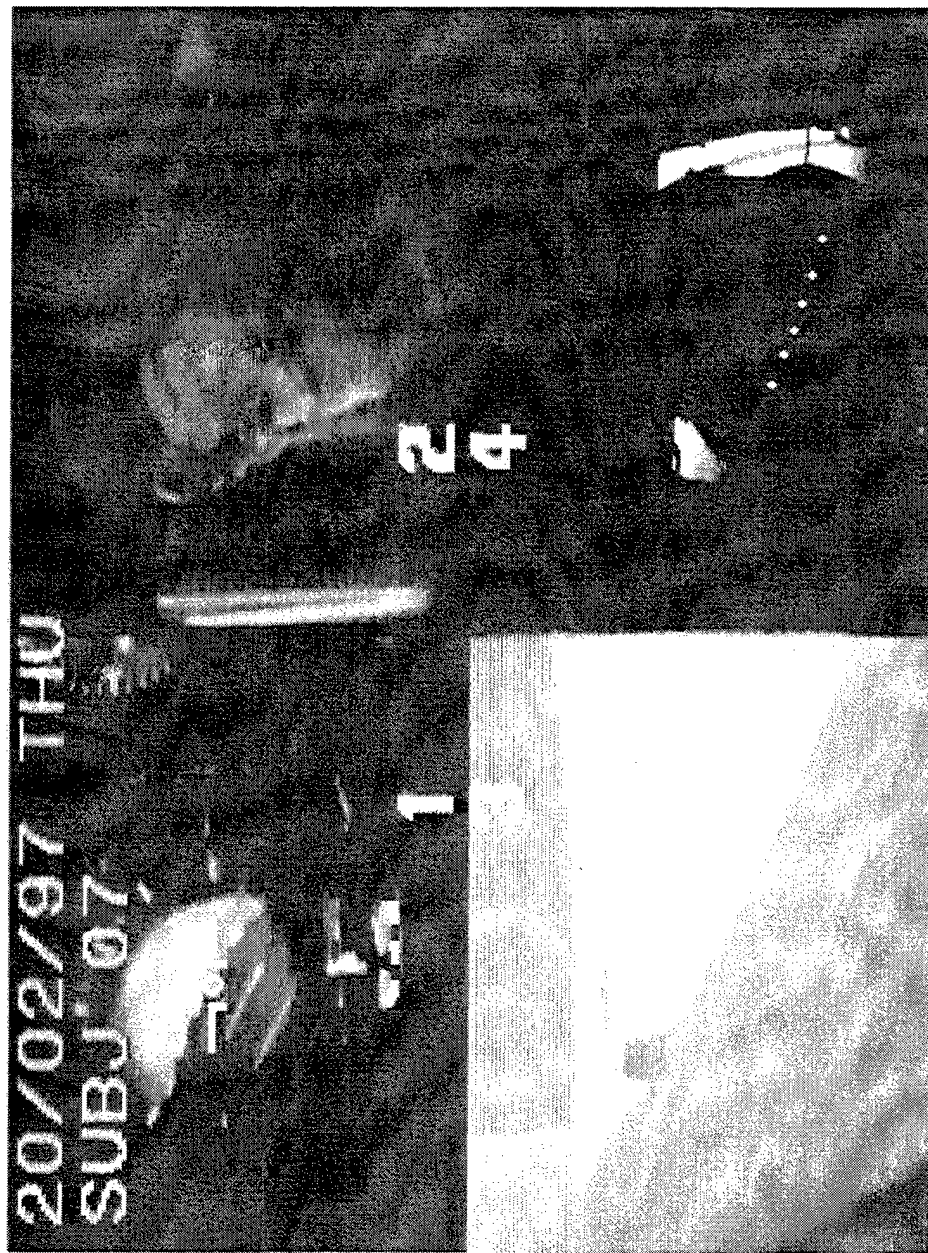


Image frame numbers refer to camera locations in figure 7. The subject is executing a 30 degree left bank. (Note: masking of the subject's eyes has been applied in this photograph to maintain confidentiality).

Figure 8. Still photograph from video recording.

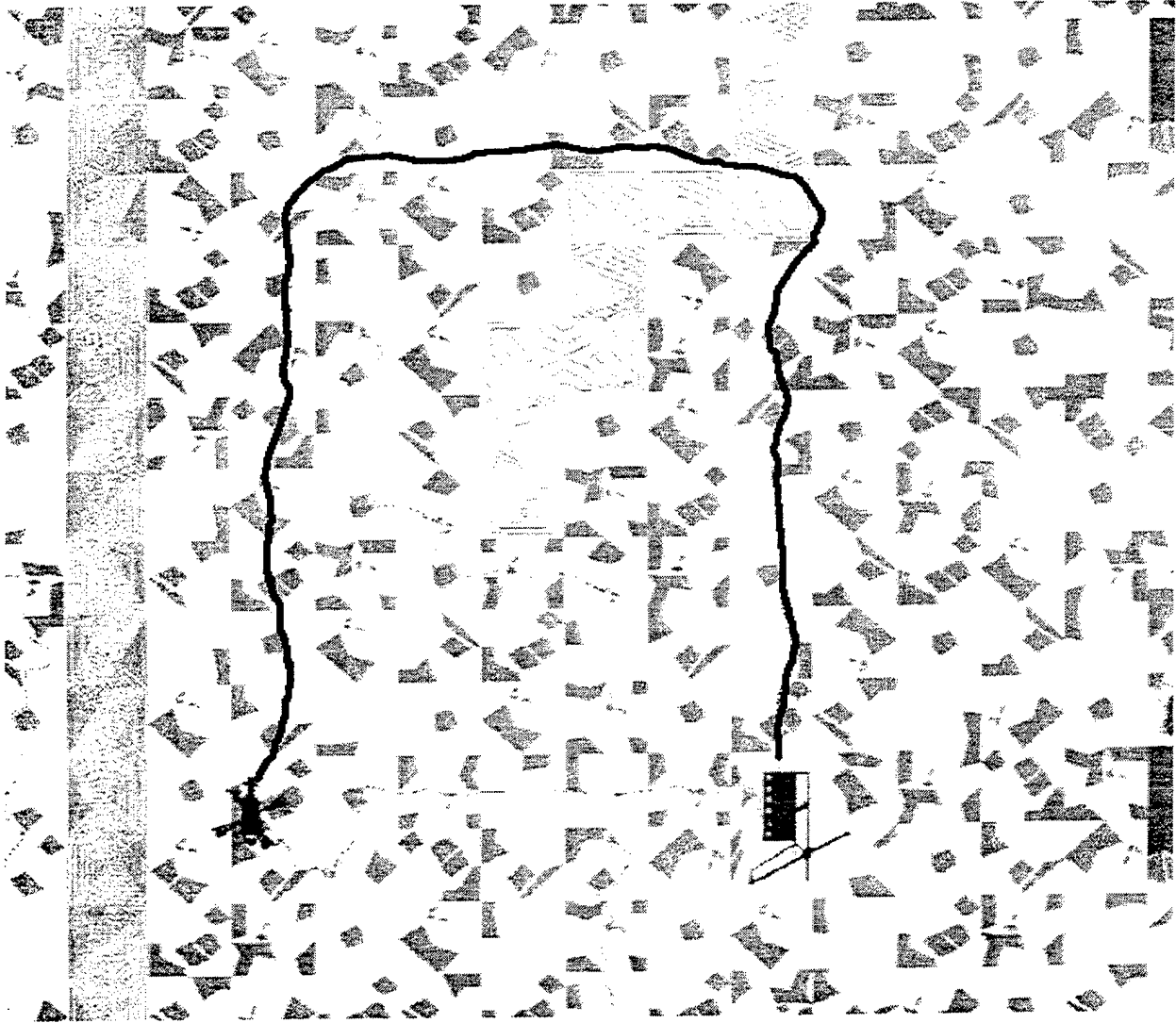


Figure 9. Ground track of task 1.

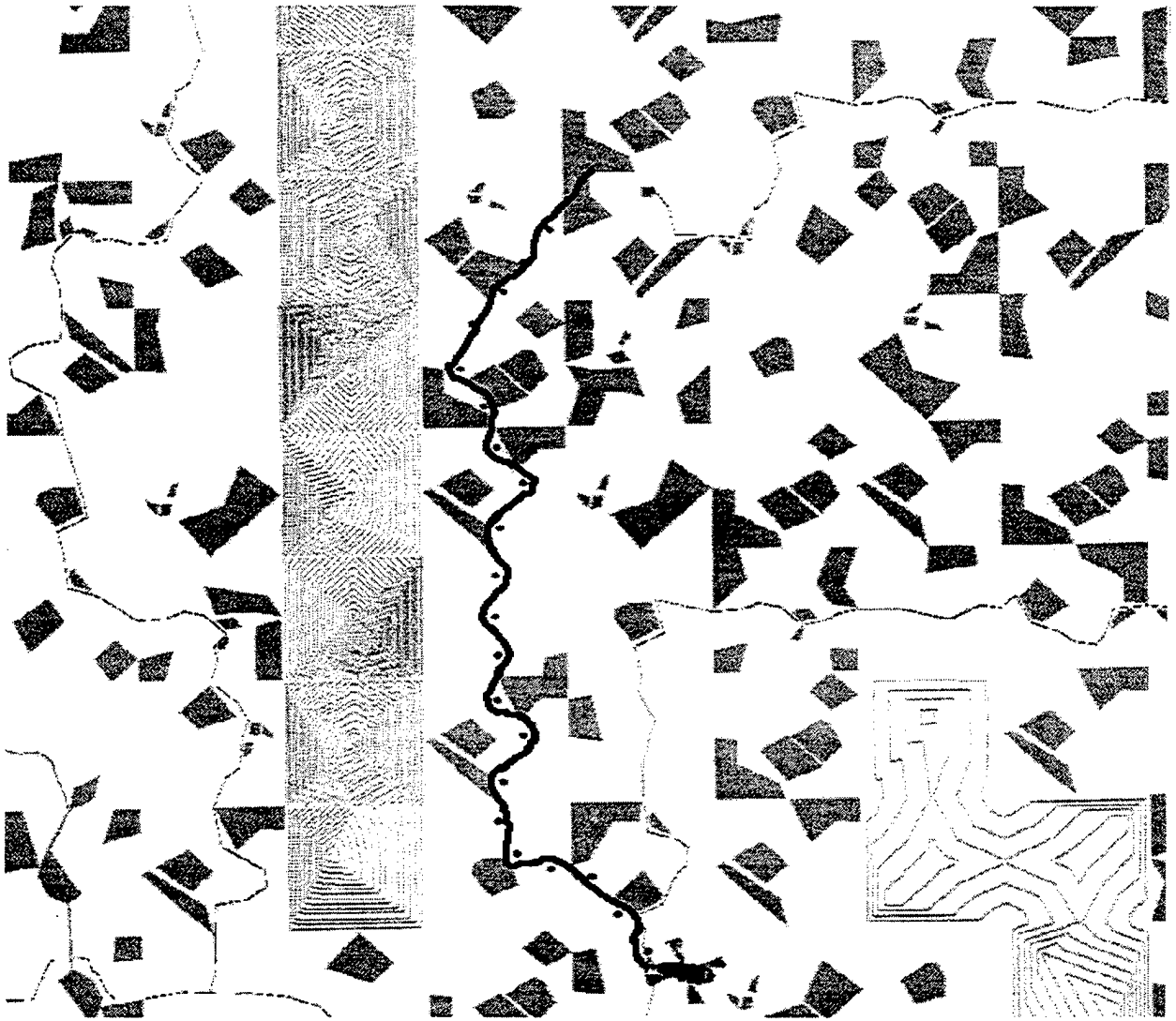


Figure 10. Ground track of task 2.

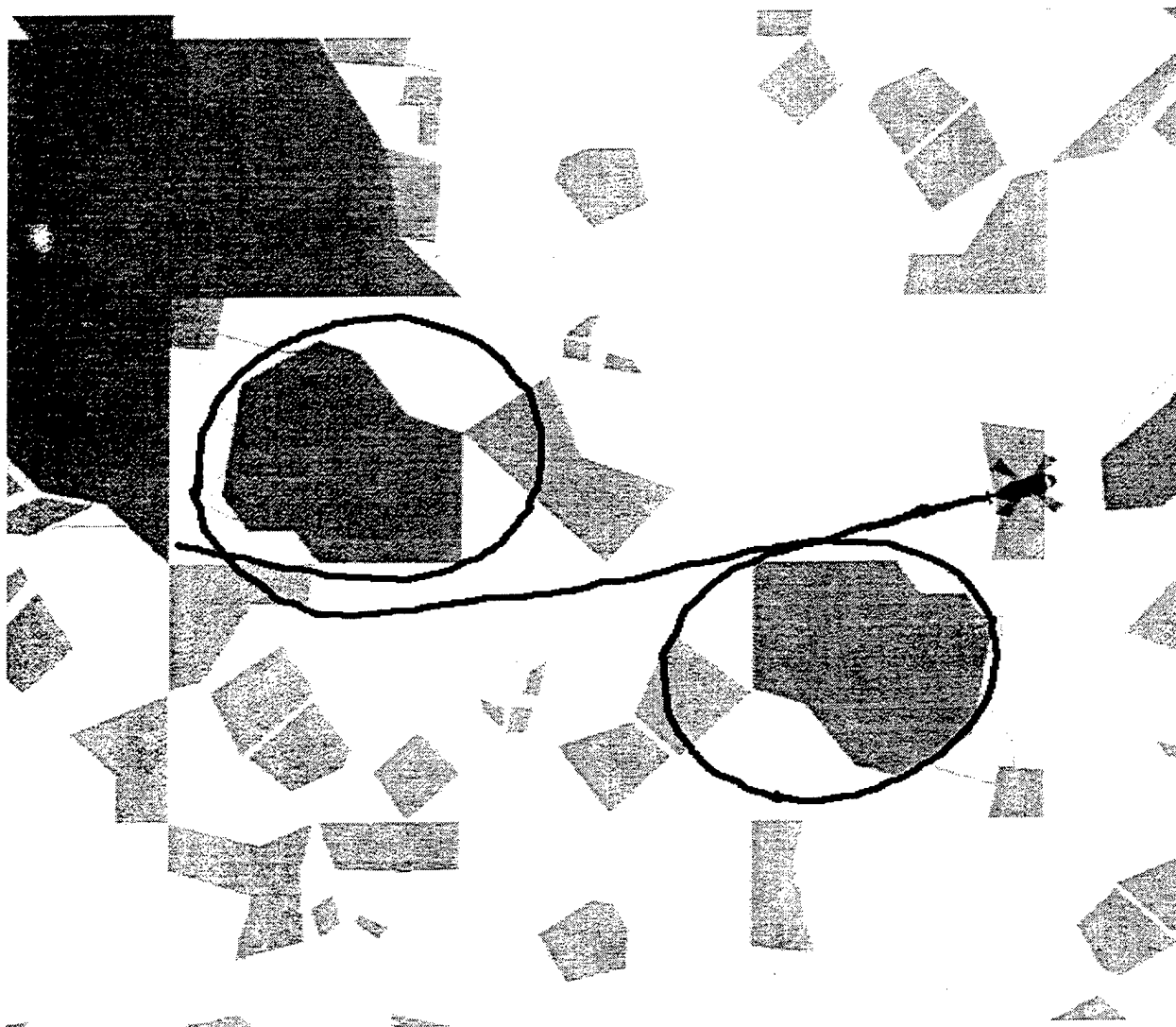


Figure 11. Ground track of task 3.

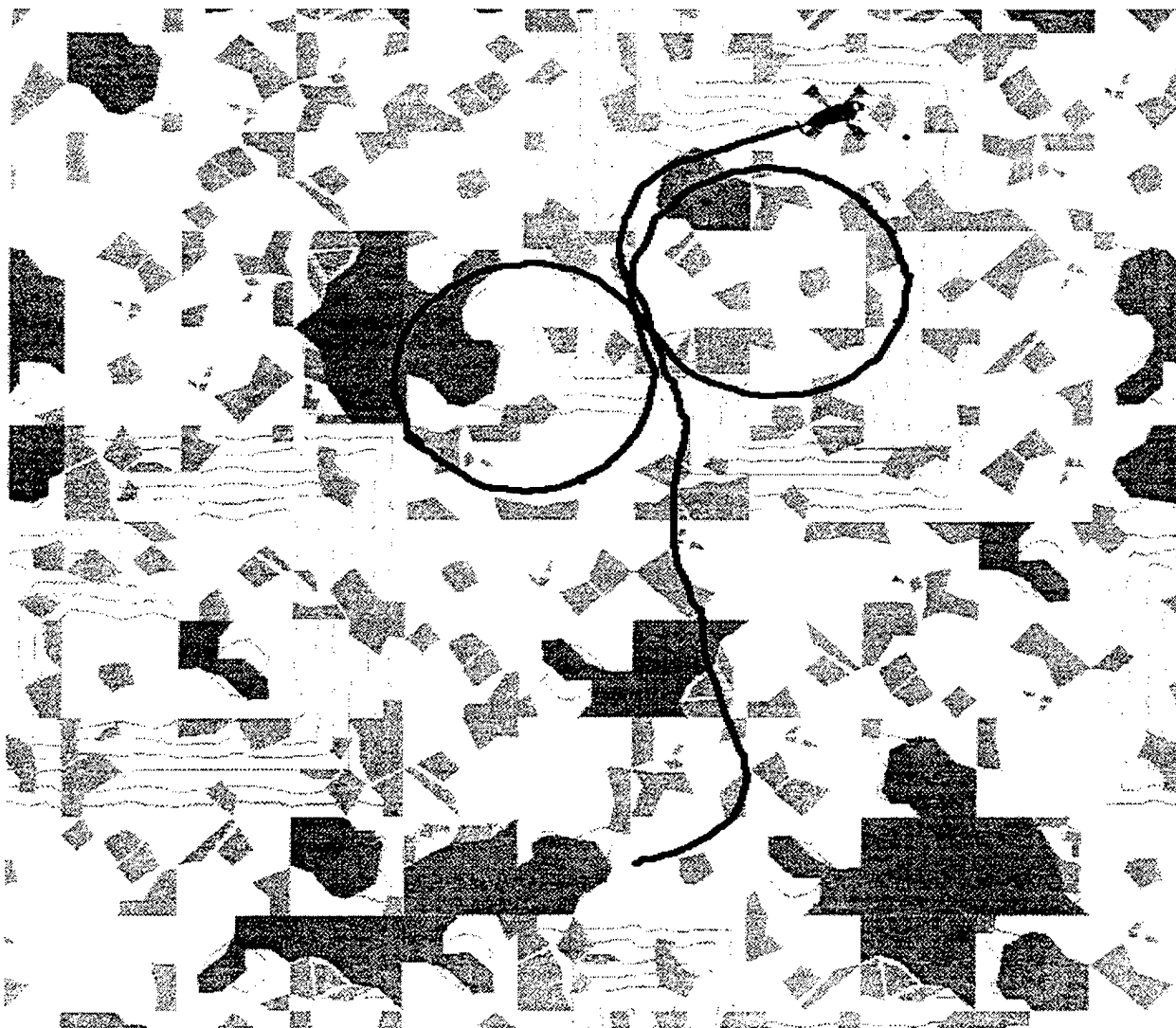


Figure 12. Ground track of task 4.

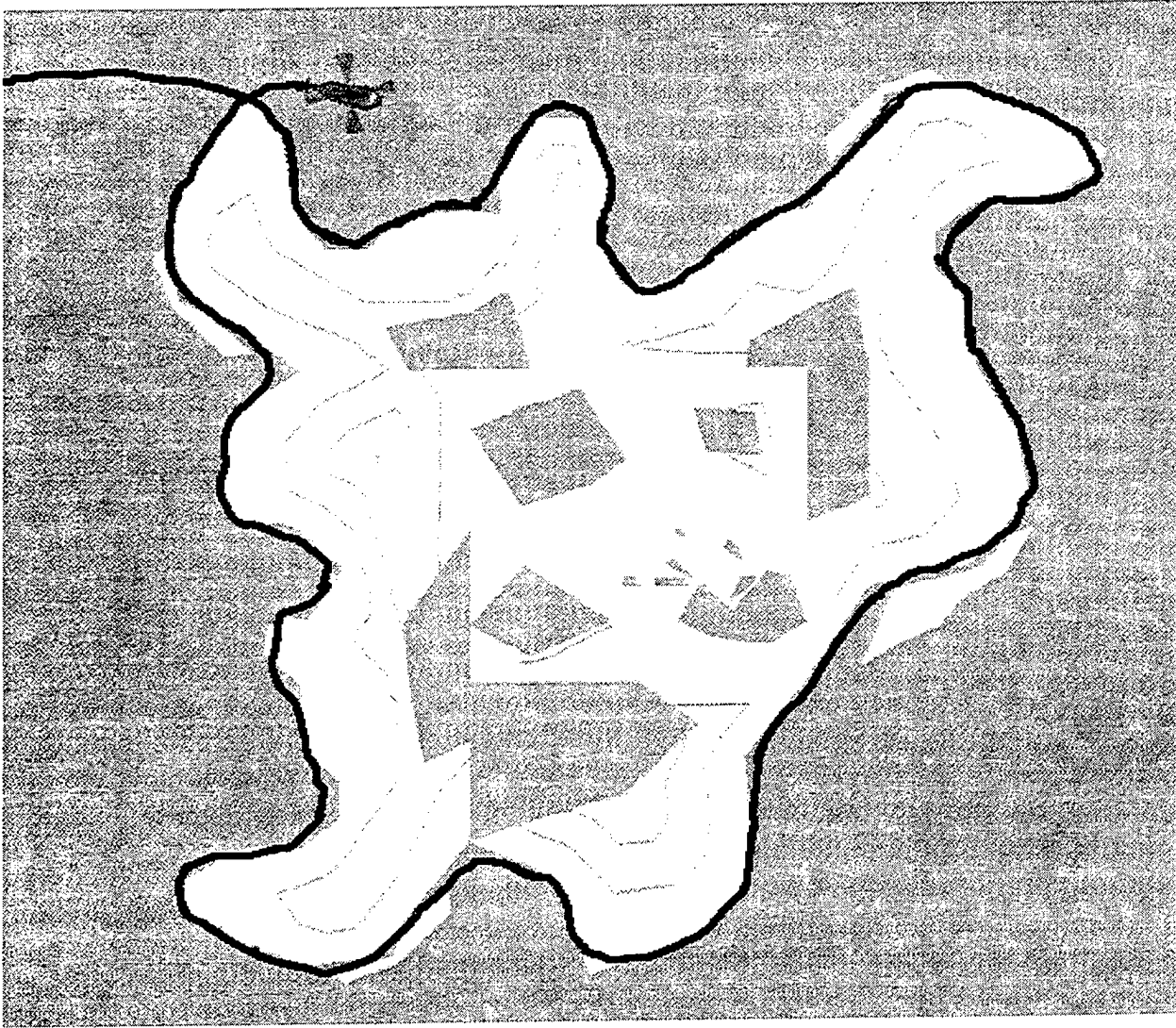


Figure 13. Ground track of task 5.

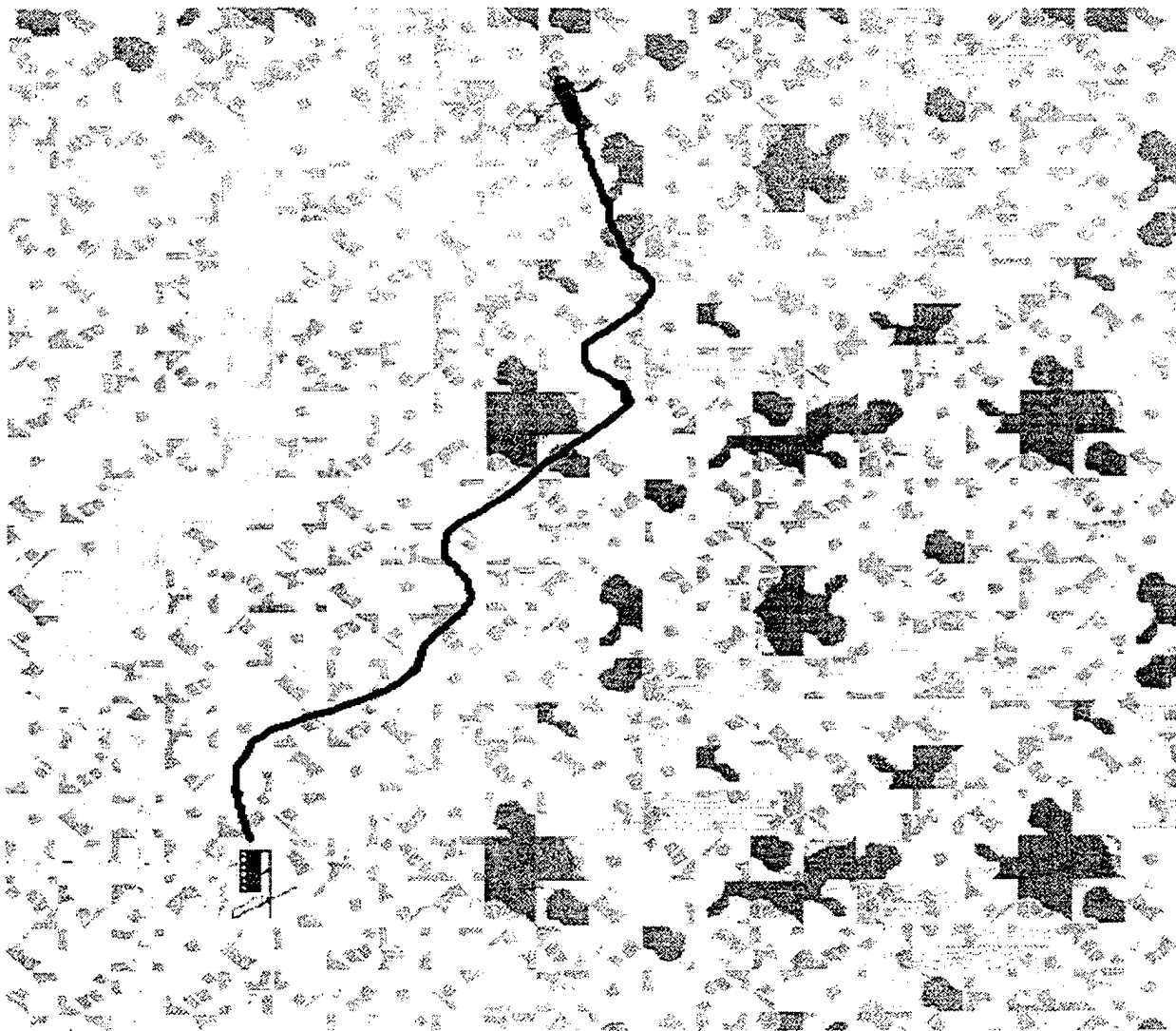


Figure 14. Ground track of task 6.

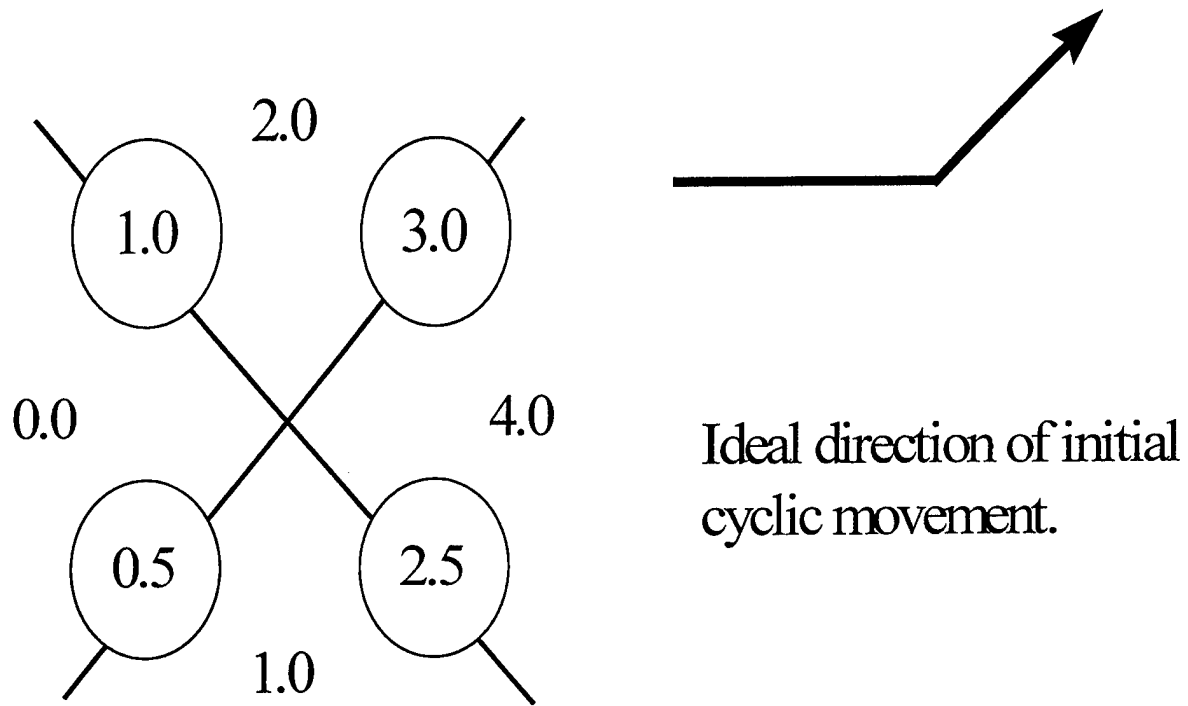


Figure 15. Scoring guide for reversal error.

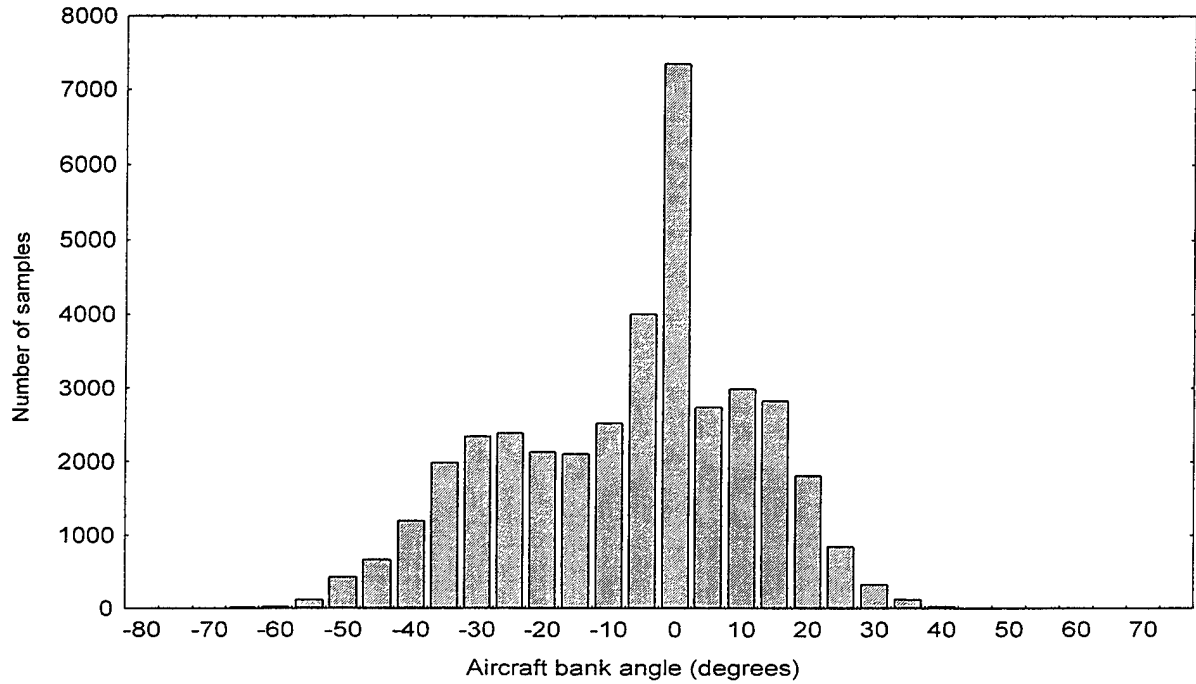


Figure 16. Histogram of task 1 (day) data sampling from all subjects for multiple levels of aircraft bank angle.

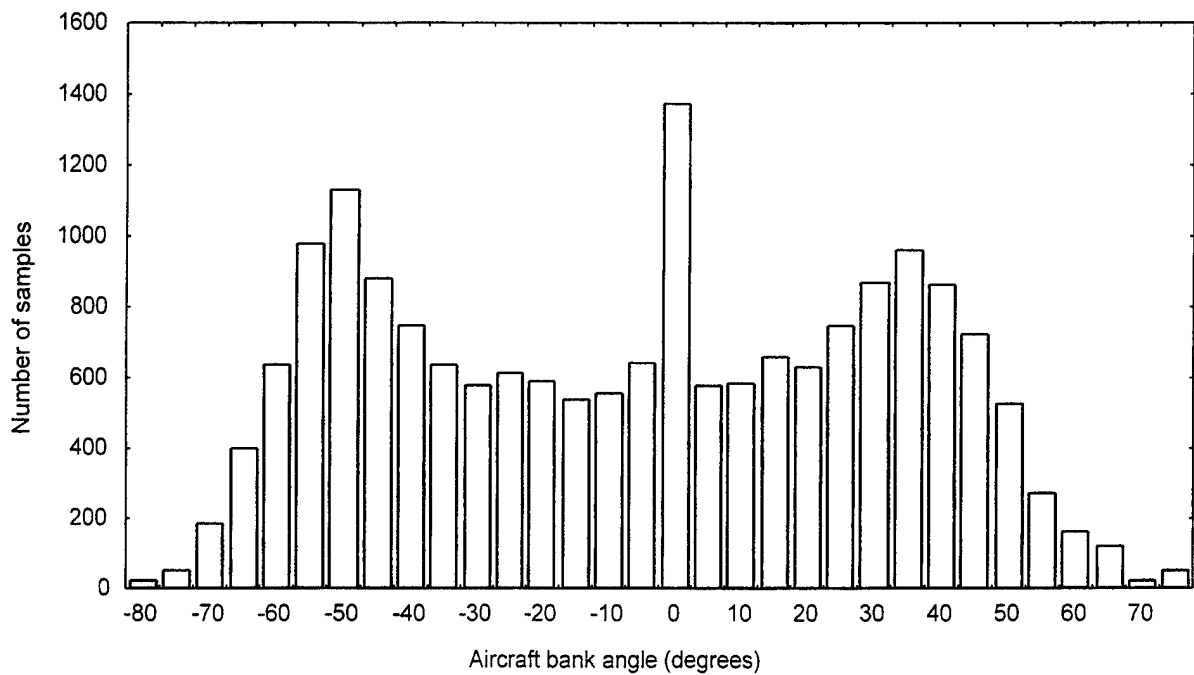


Figure 17. Histogram of task 2 (day) data sampling from all subjects for multiple levels of aircraft bank angle.

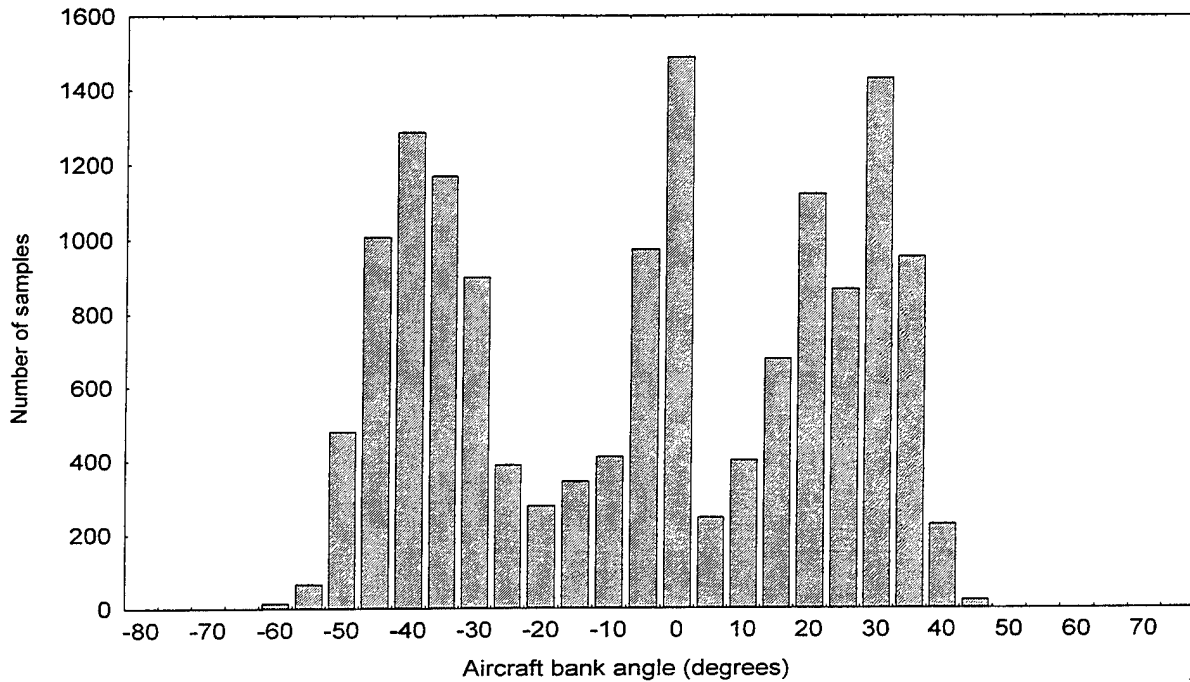


Figure 18. Histogram of task 3 (day) data sampling from all subjects for multiple levels of aircraft bank angle.

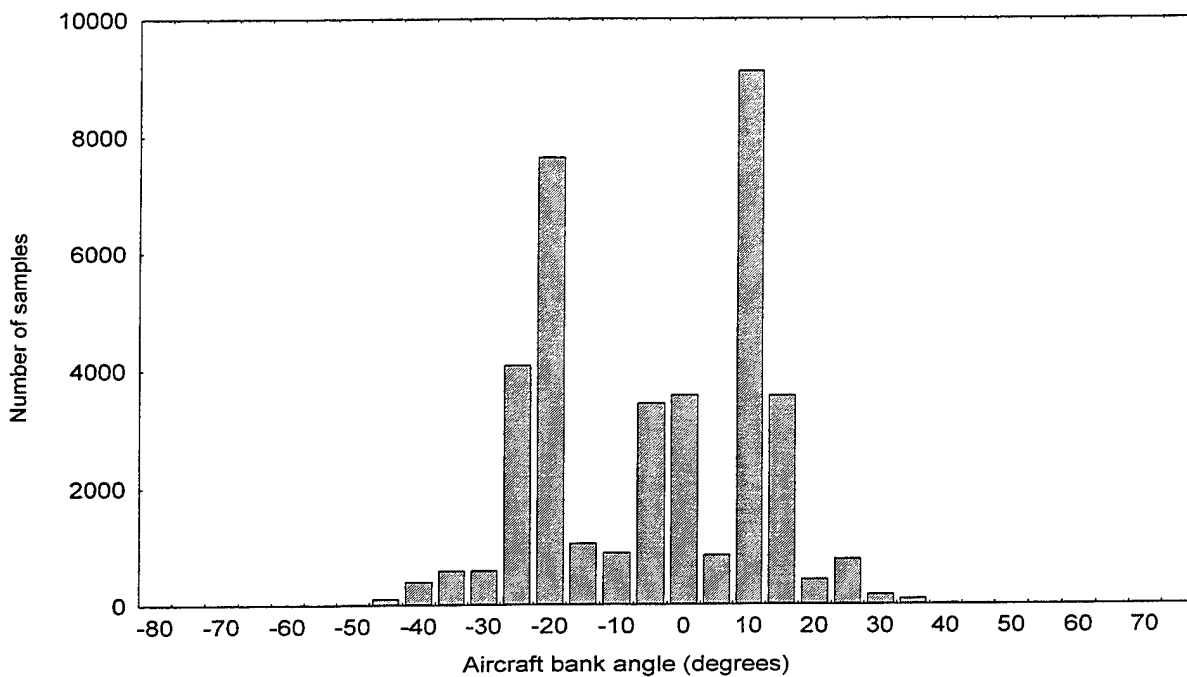


Figure 19. Histogram of task 4 (day) data sampling from all subjects for multiple levels of aircraft bank angle.

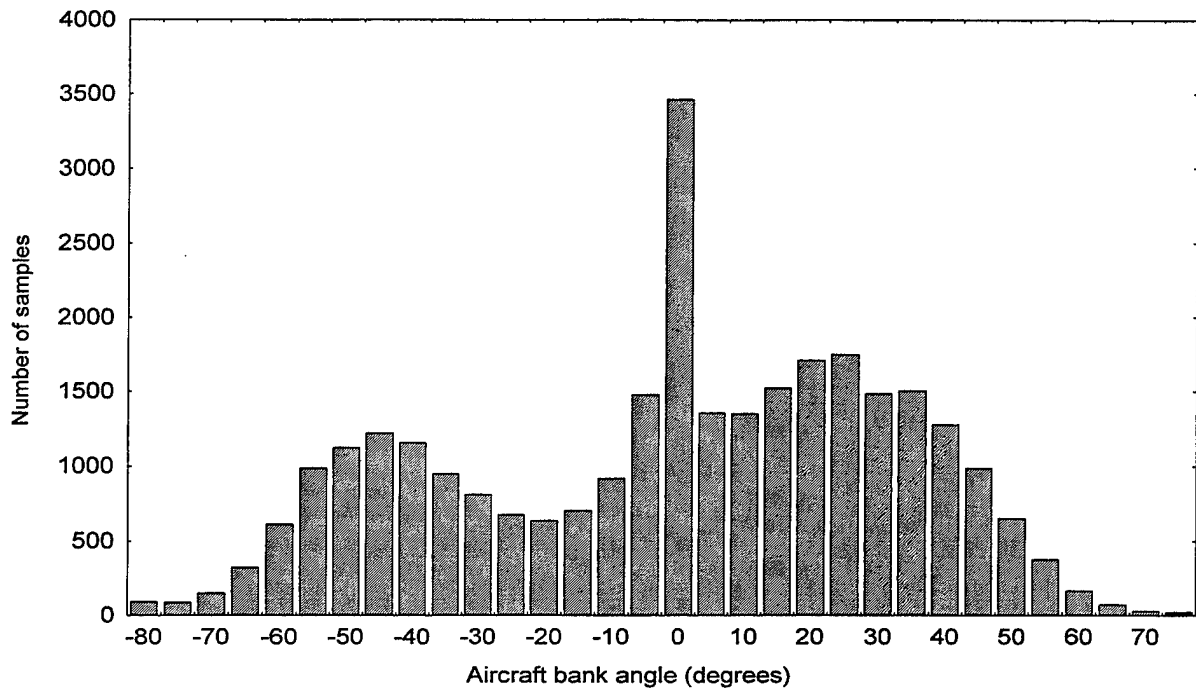


Figure 20. Histogram of task 5 (day) data sampling from all subjects for multiple levels of aircraft bank angle.

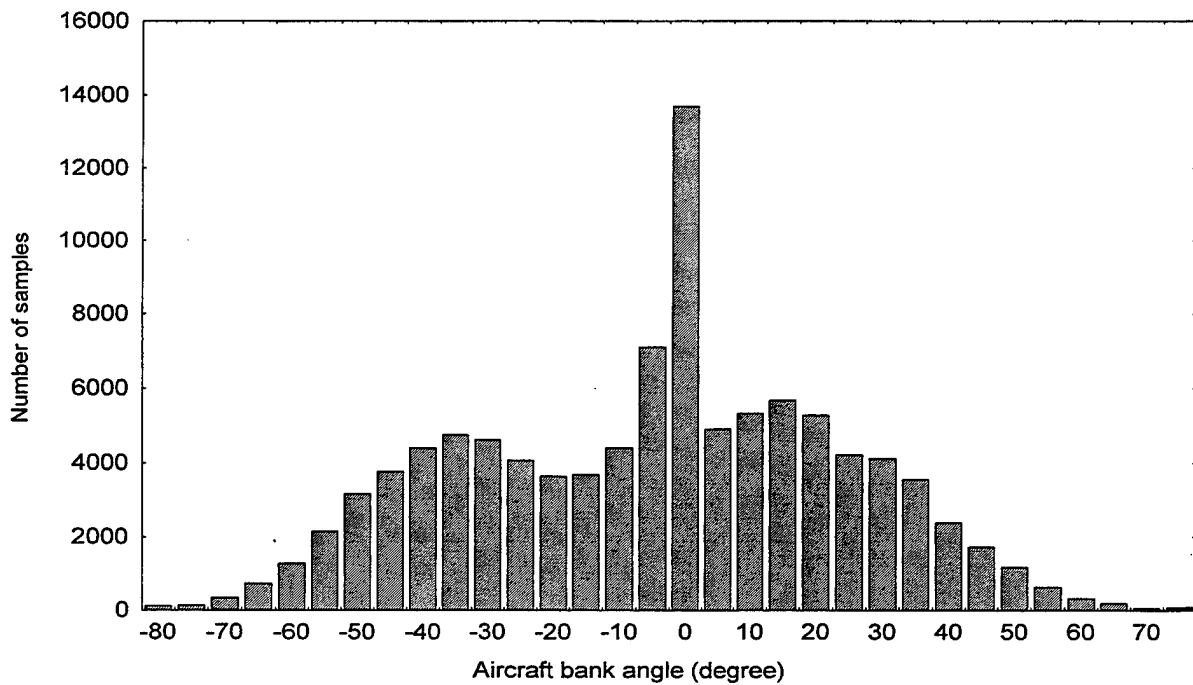


Figure 21. Histogram of task 7 (day) data sampling from all subjects for multiple levels of aircraft bank angle.

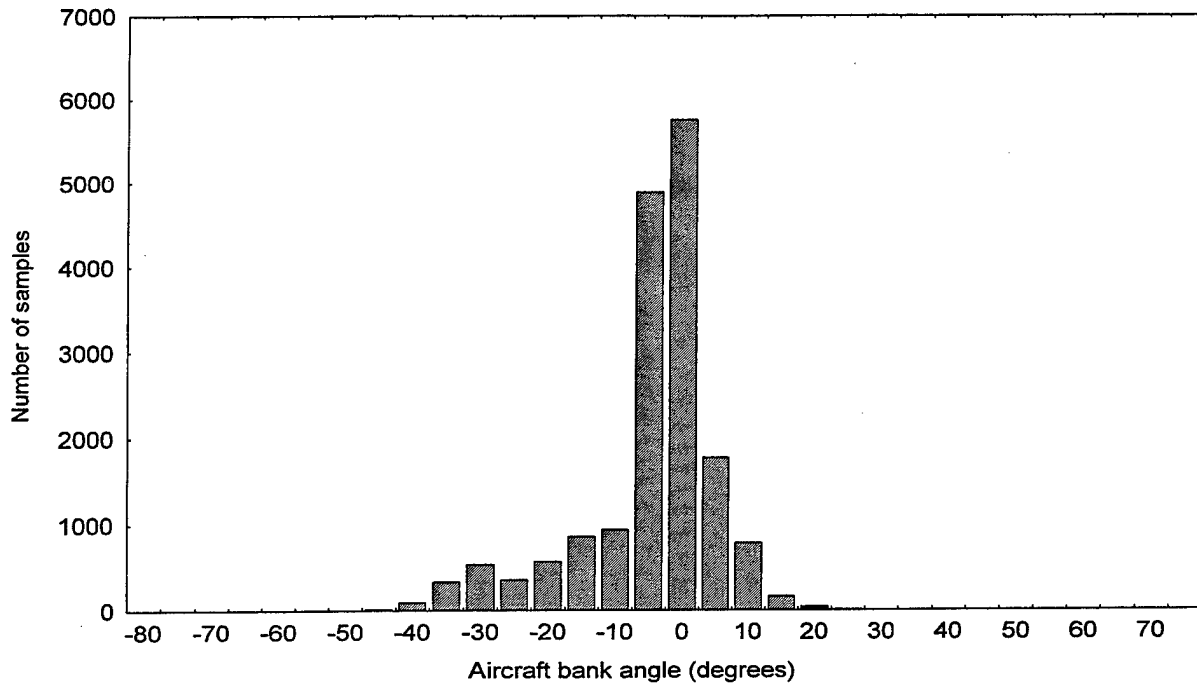


Figure 22. Histogram of task 6y (day) data sampling from all subjects for multiple levels of aircraft bank angle.

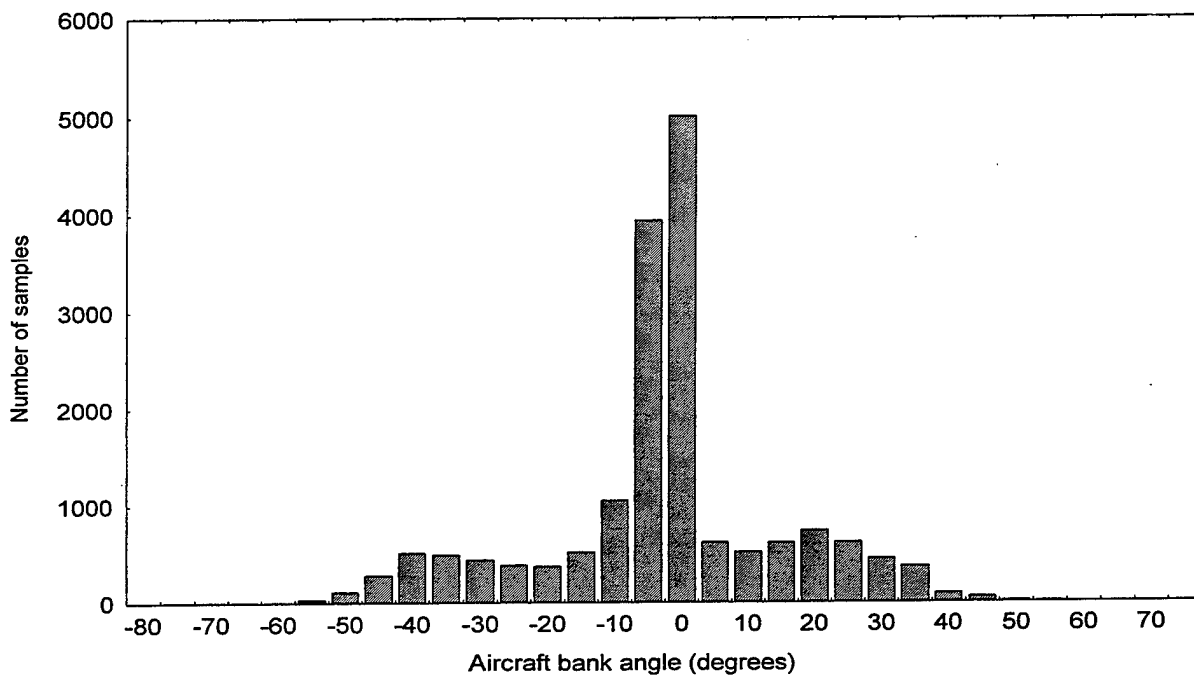


Figure 23. Histogram of task 6z (day) data sampling from all subjects for multiple levels of aircraft bank angle.

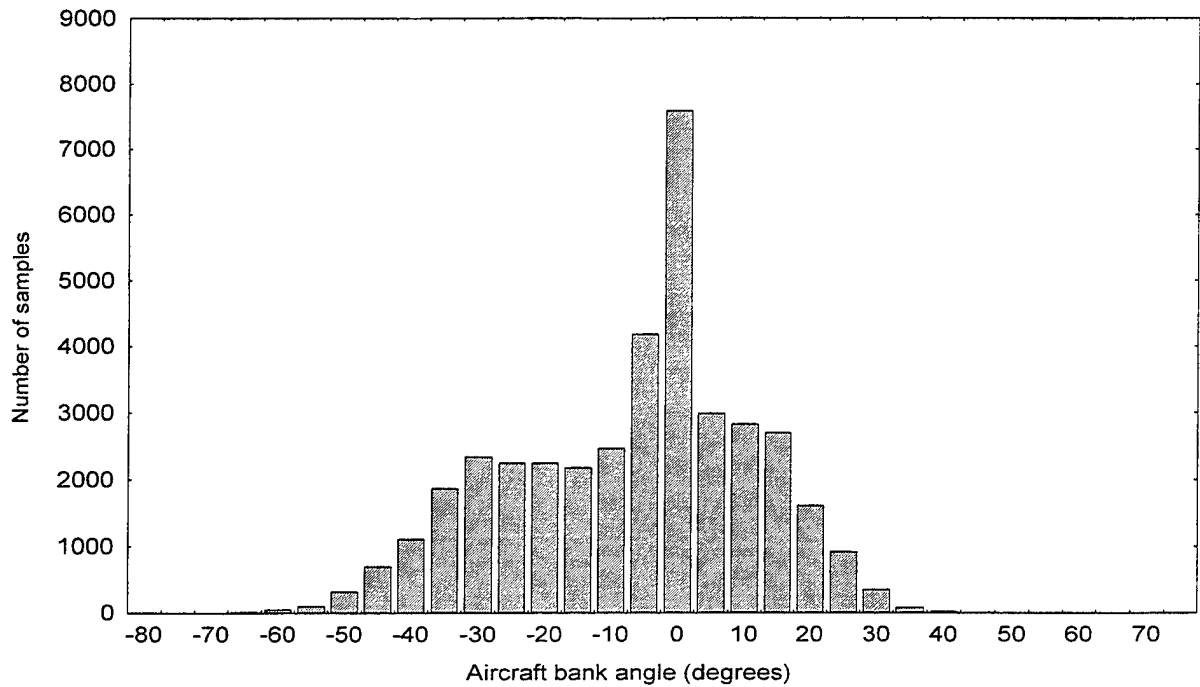


Figure 24. Histogram of task 1 (night) data sampling from all subjects for multiple levels of aircraft bank angle.

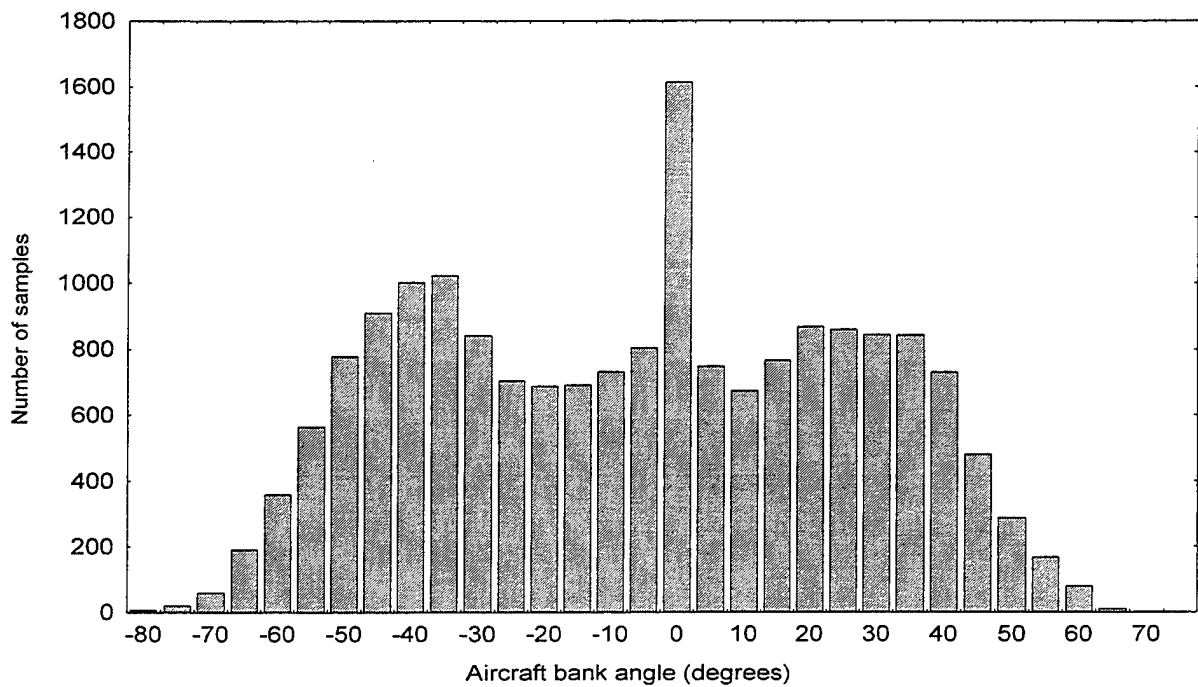


Figure 25. Histogram of task 2 (night) data sampling from all subjects for multiple levels of aircraft bank angle.

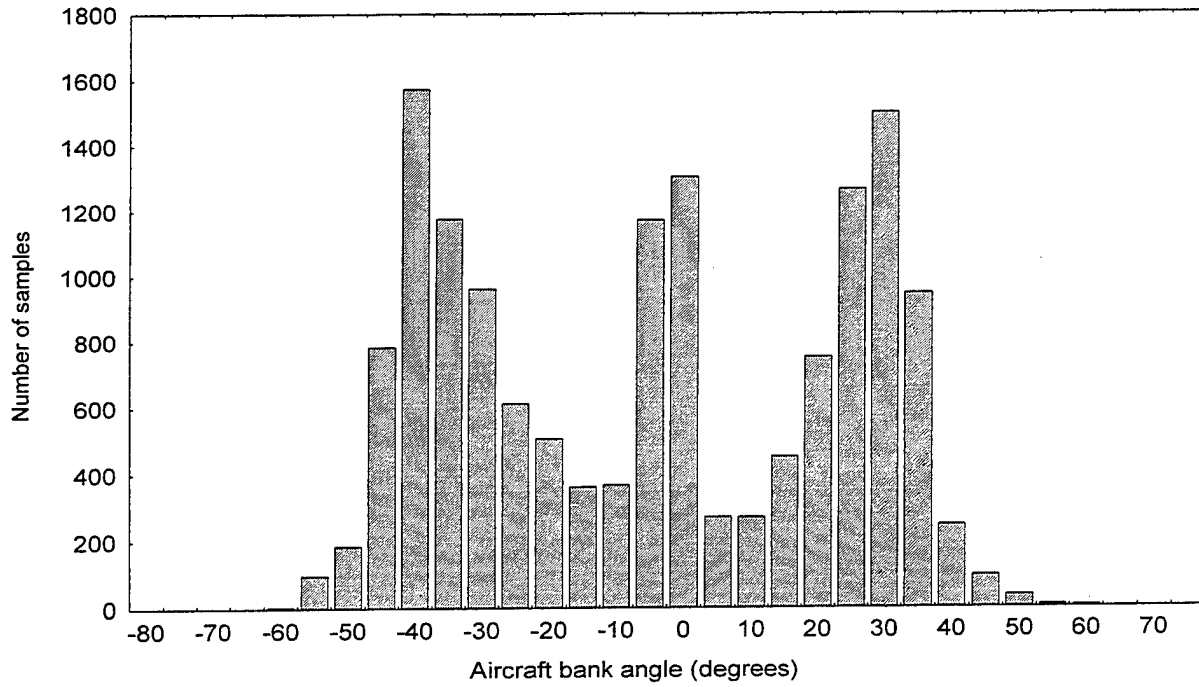


Figure 26. Histogram of task 3 (night) data sampling from all subjects for multiple levels of aircraft bank angle.

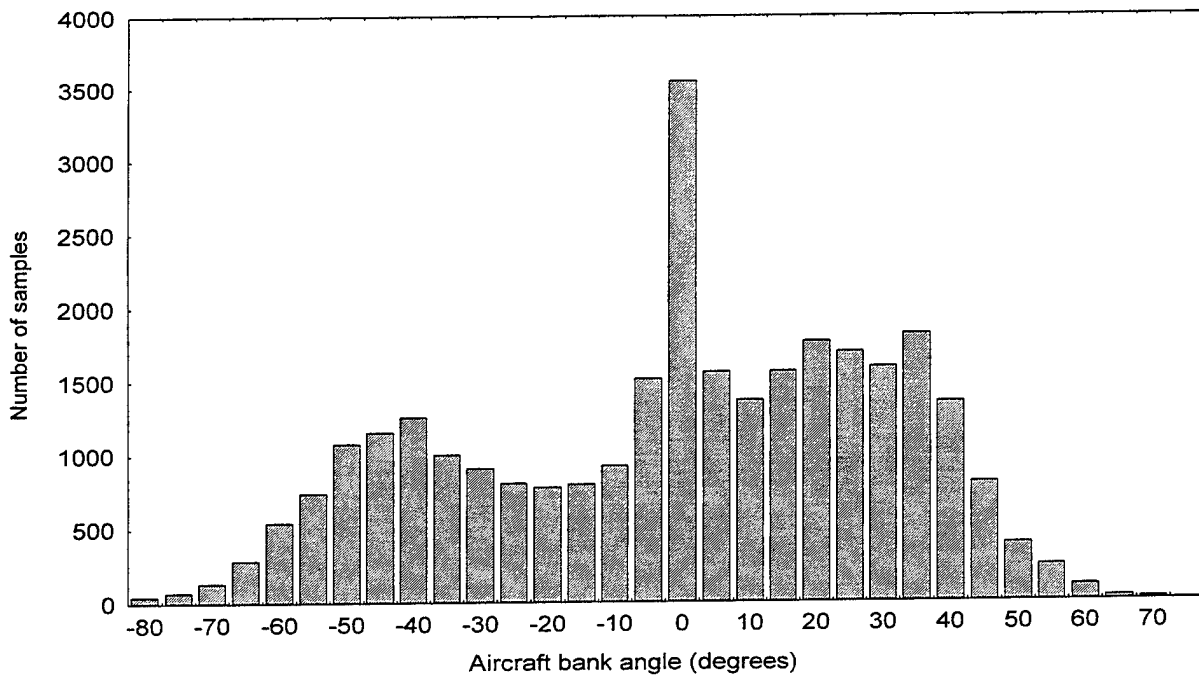


Figure 27. Histogram of task 5 (night) data sampling from all subjects for multiple levels of aircraft bank angle.

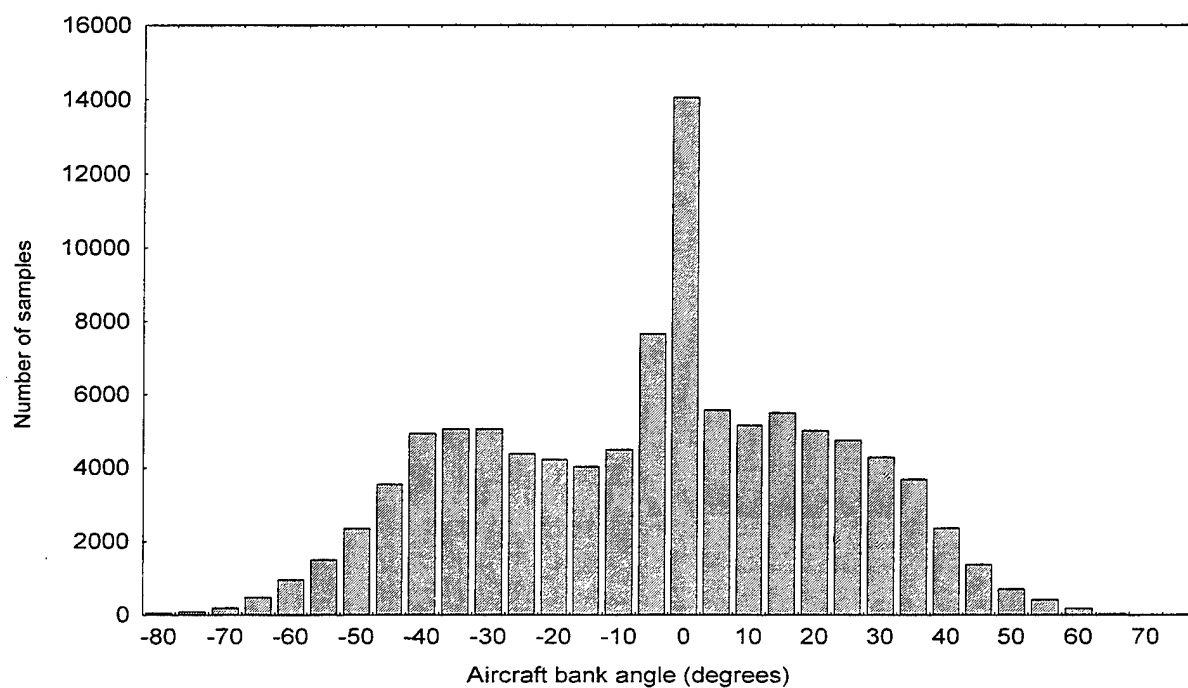


Figure 28. Histogram of task 7 (night) data sampling from all subjects for multiple levels of aircraft bank angle.

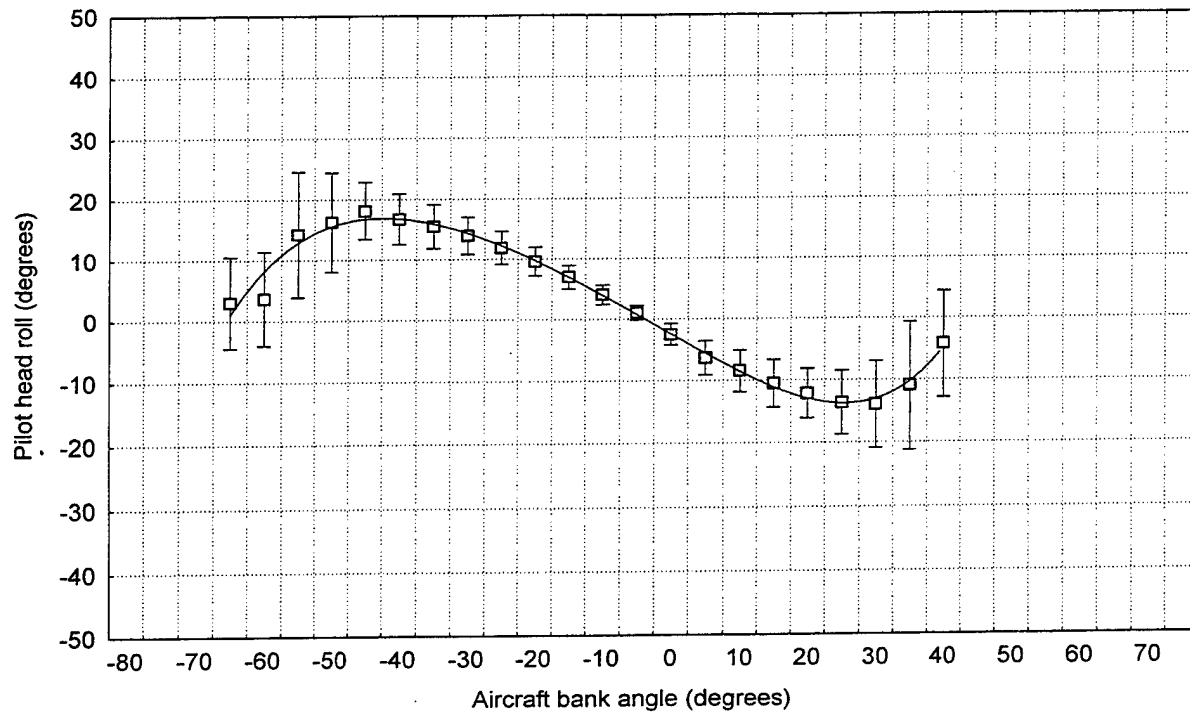


Figure 29. Mean (± 1 SD) head roll as a function of aircraft bank angle. Task 1, day.

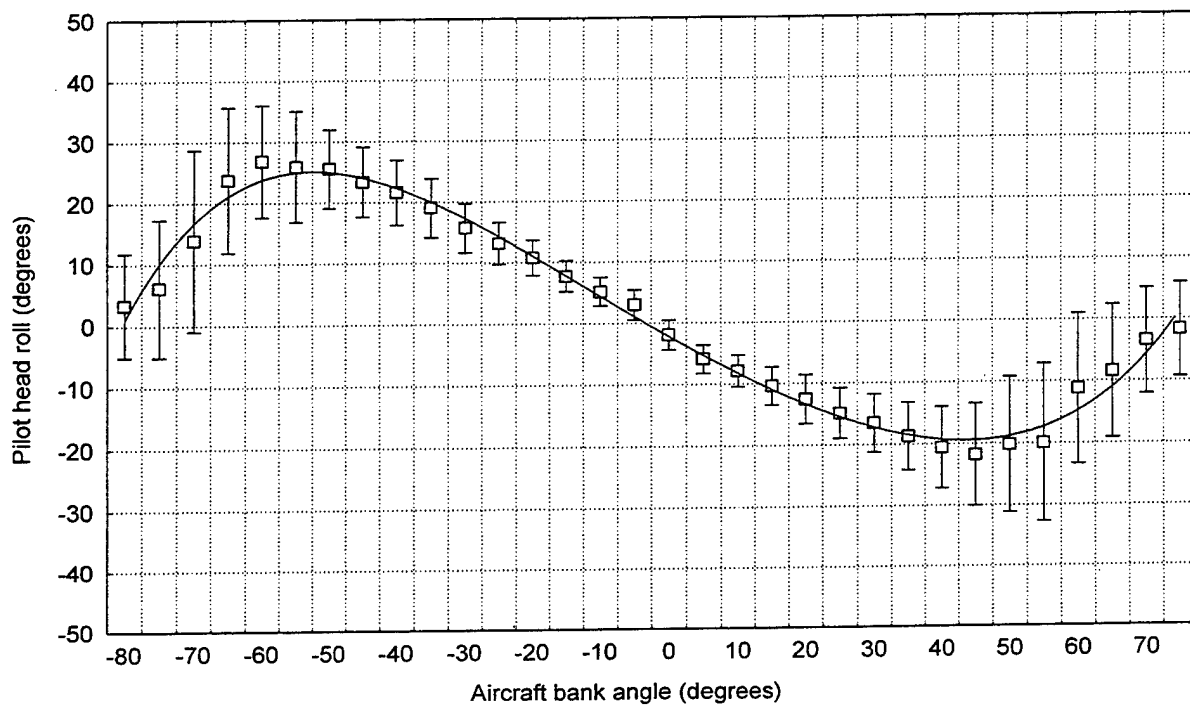


Figure 30. Mean (± 1 SD) head roll as a function of aircraft bank angle. Task 2, day.

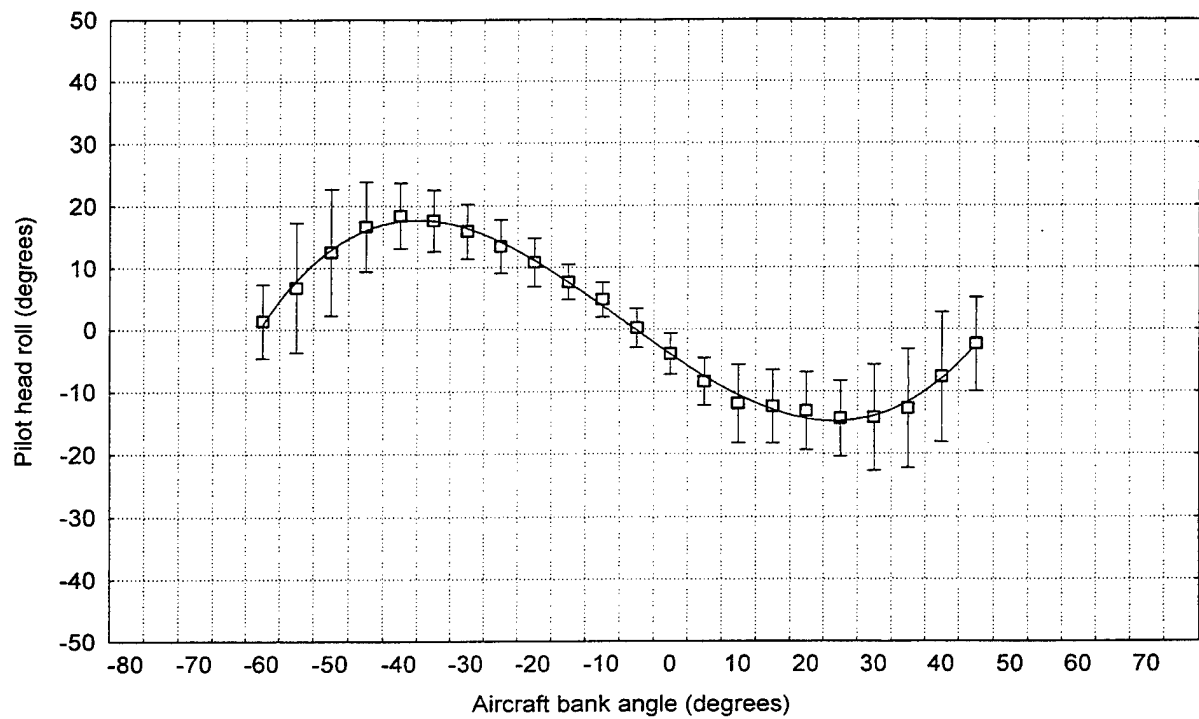


Figure 31. Mean (± 1 SD) head roll as a function of aircraft bank angle. Task 3, day.

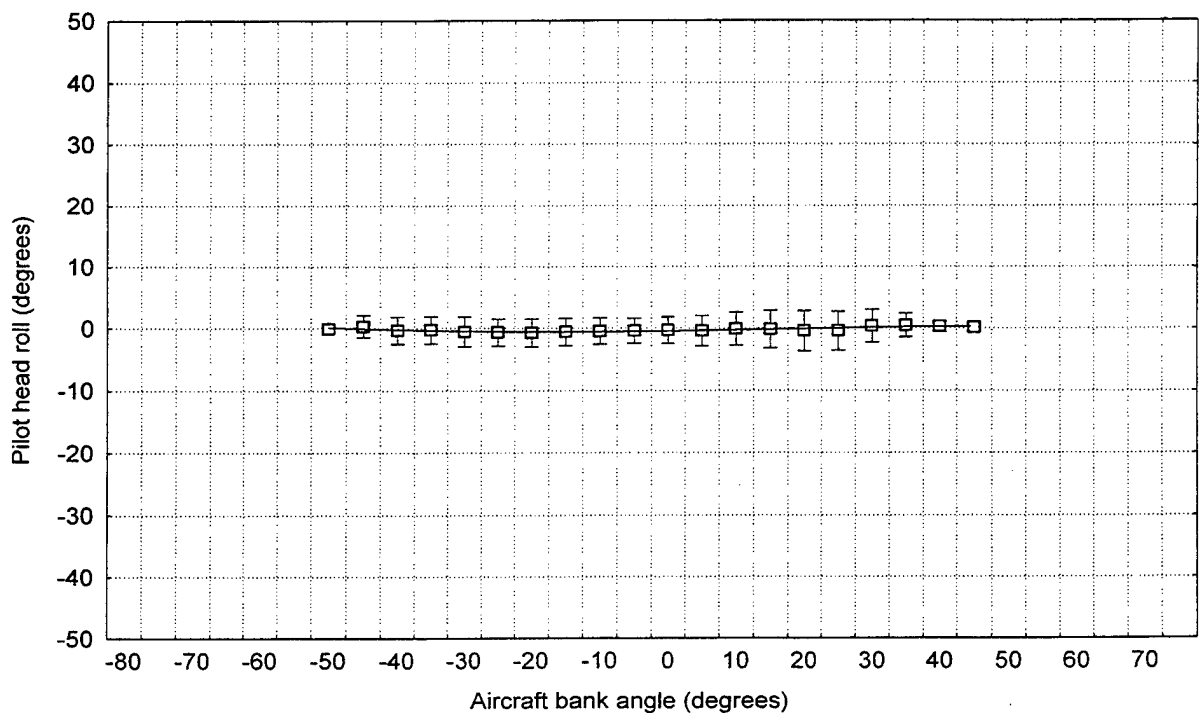


Figure 32. Mean (± 1 SD) head roll as a function of aircraft bank angle. Task 4, day.

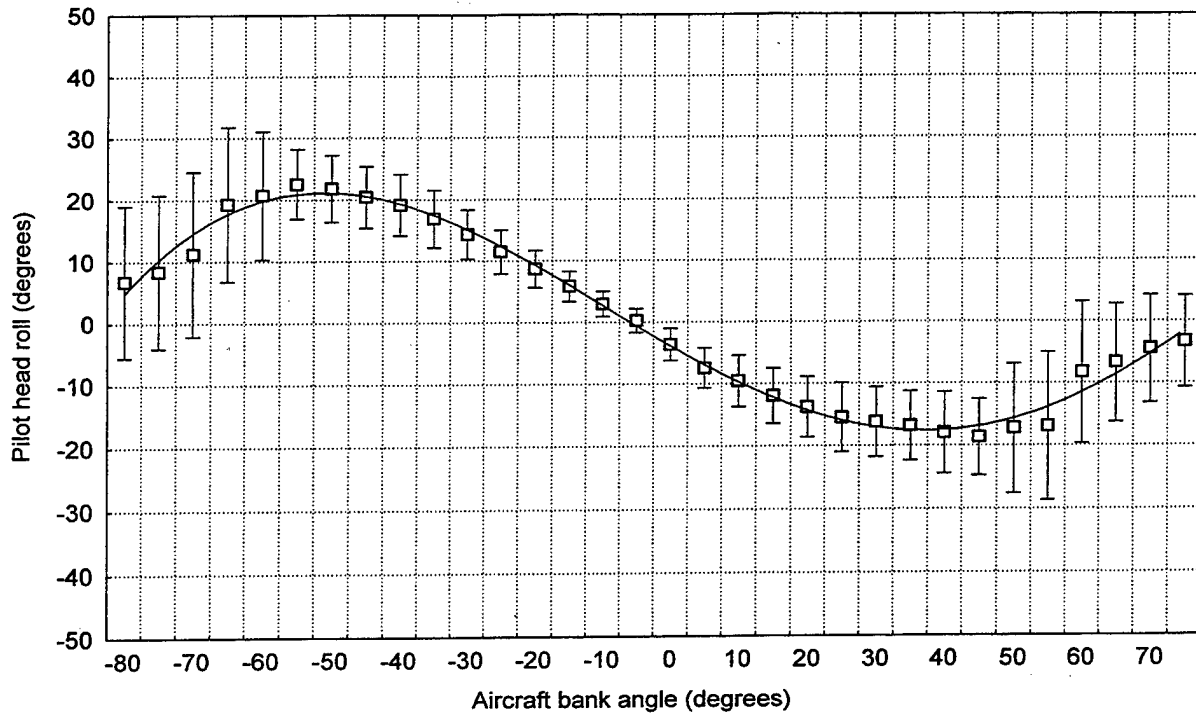


Figure 33. Mean (± 1 SD) head roll as a function of aircraft bank angle. Task 5, day.

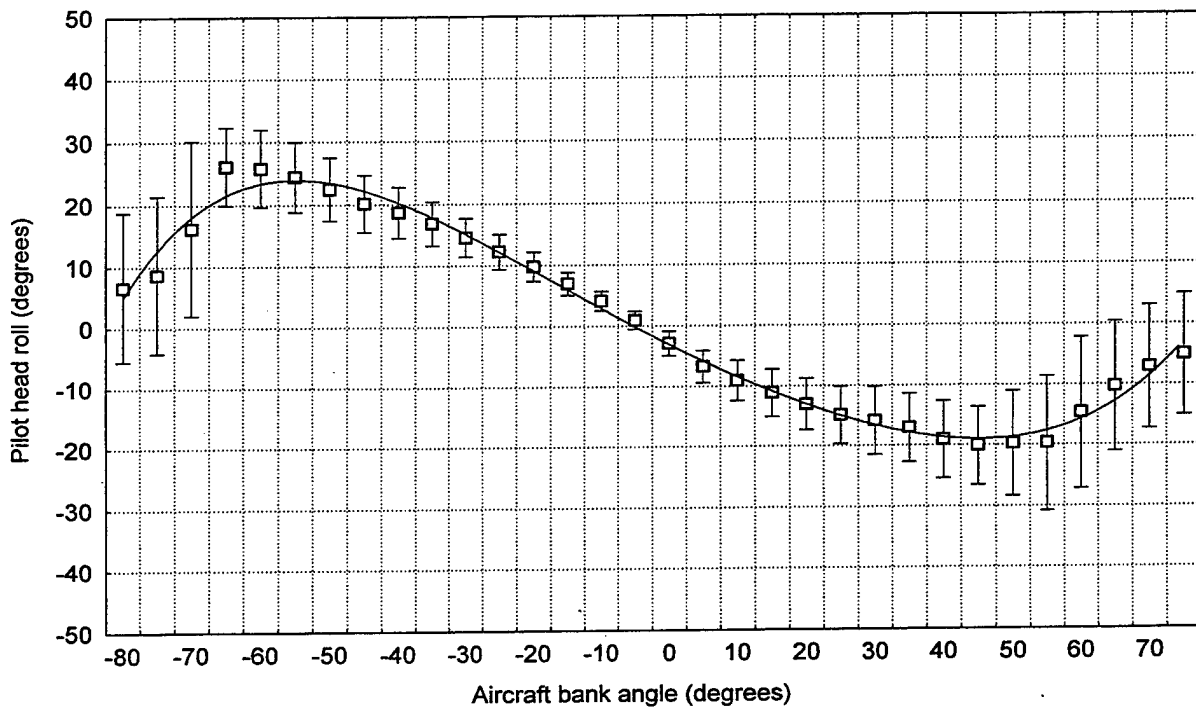


Figure 34. Mean (± 1 SD) head roll as a function of aircraft bank angle. Task 7, day.

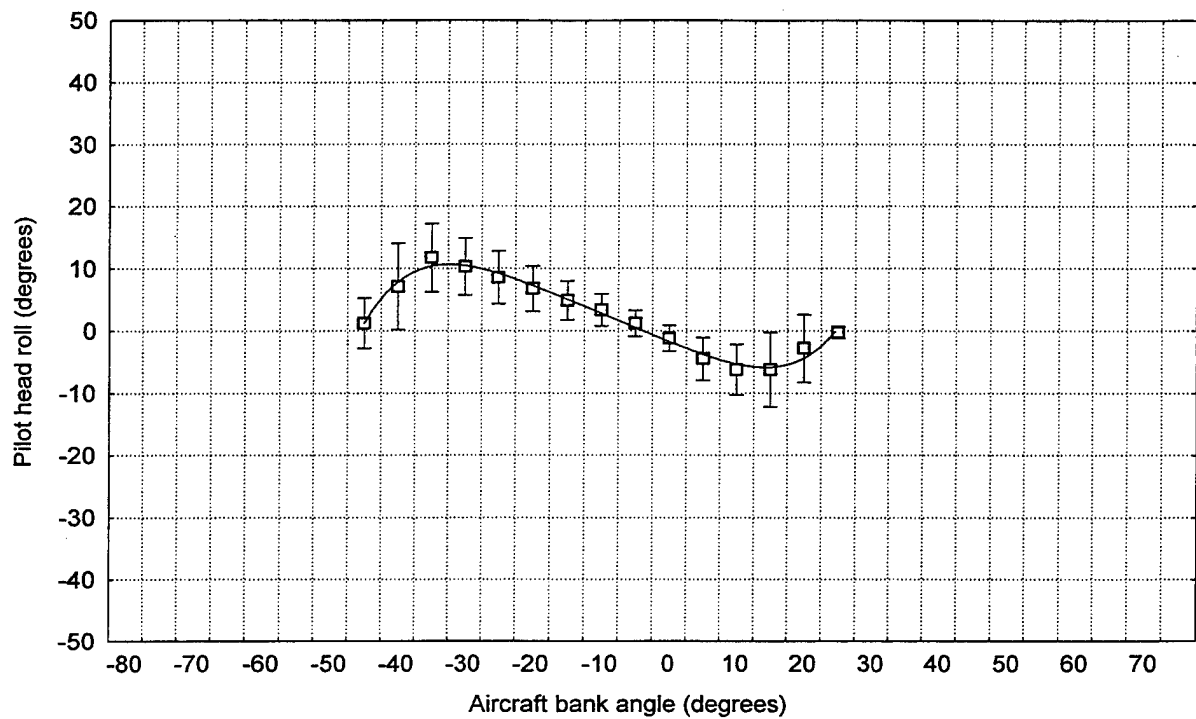


Figure 35. Mean (± 1 SD) head roll as a function of aircraft bank angle. Task 6y, day.

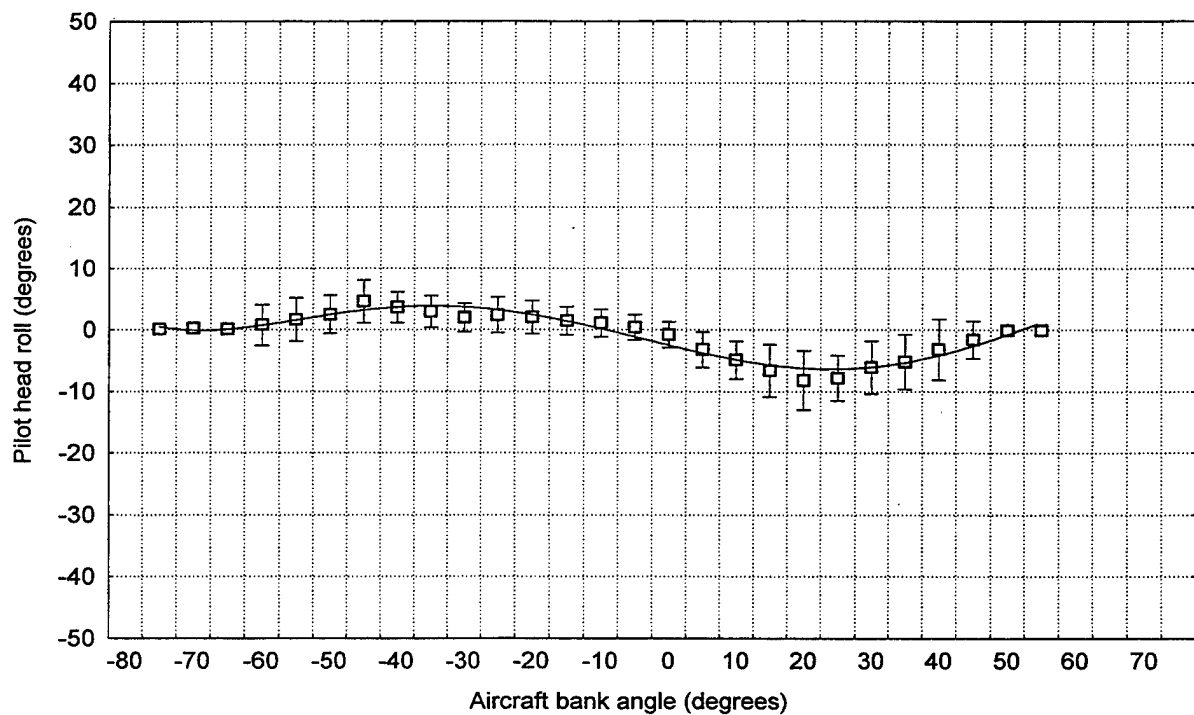


Figure 36. Mean (± 1 SD) head roll as a function of aircraft bank angle. Task 6z, day.

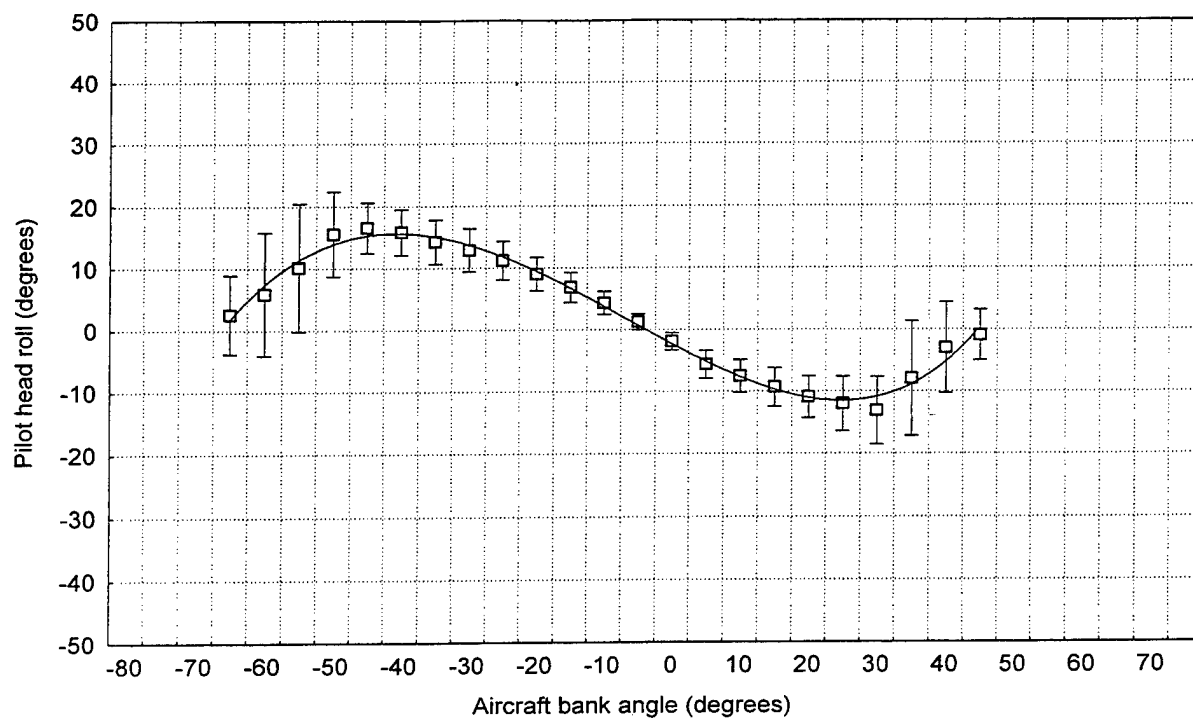


Figure 37. Mean (± 1 SD) head roll as a function of aircraft bank angle. Task 1, night.

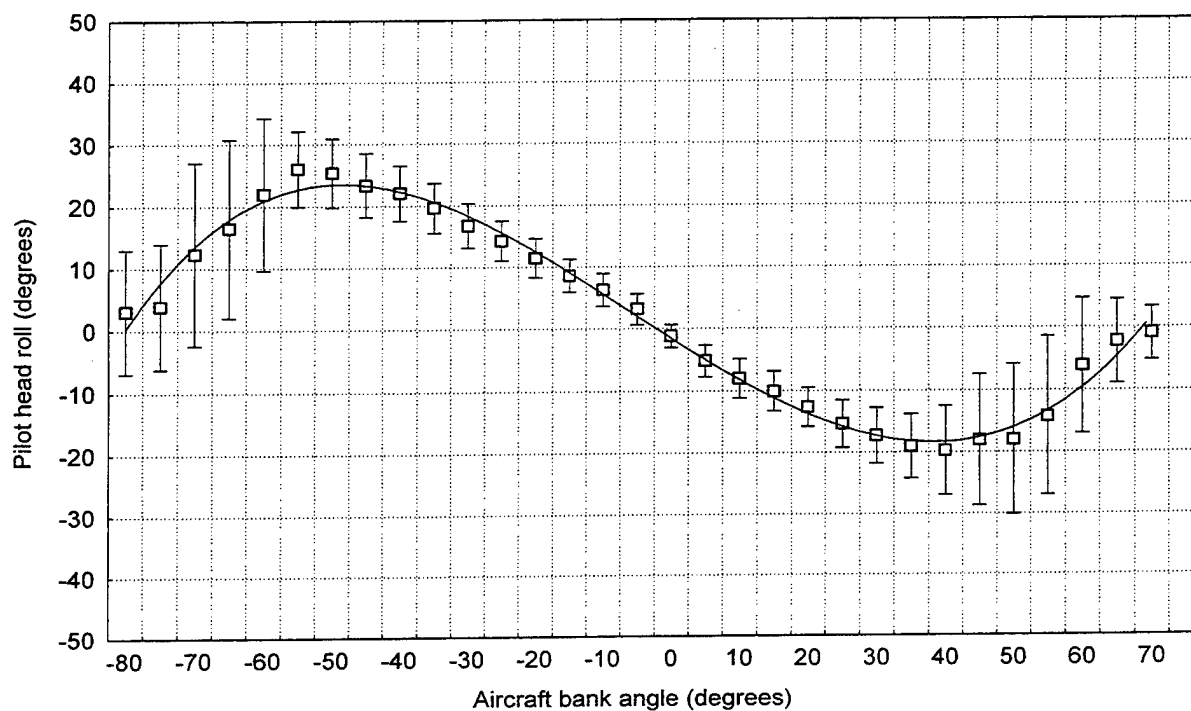


Figure 38. Mean (± 1 SD) head roll as a function of aircraft bank angle. Task 2, night.

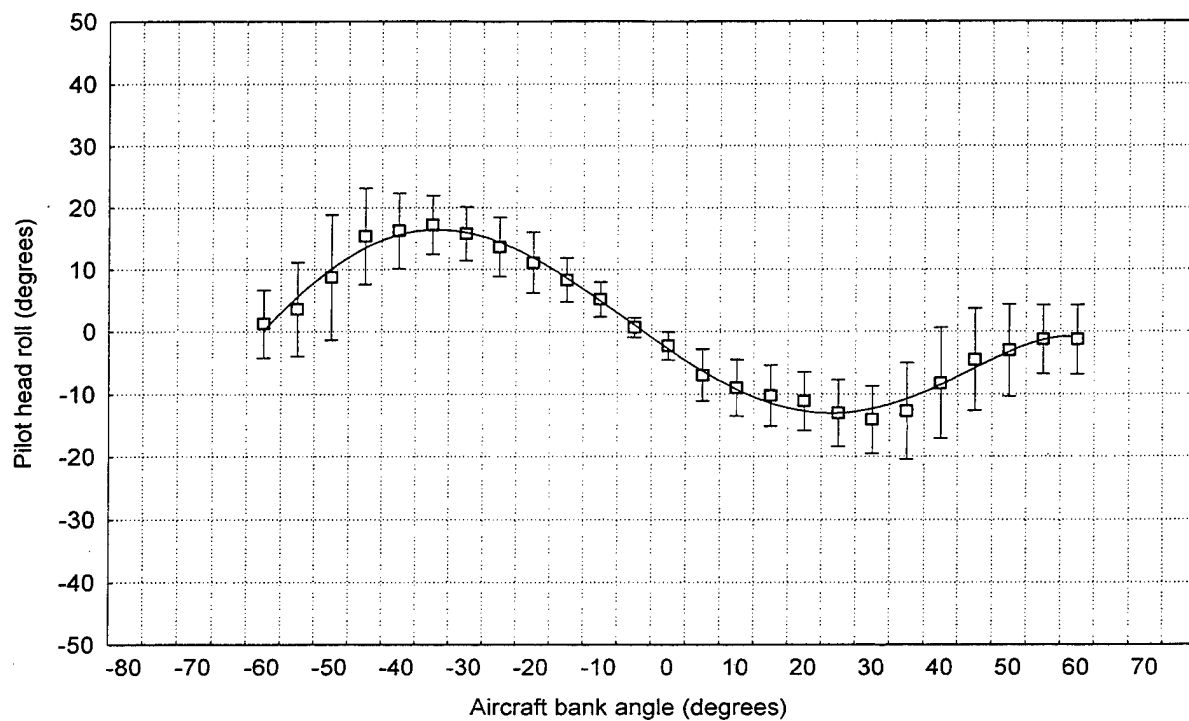


Figure 39. Mean (± 1 SD) head roll as a function of aircraft bank angle. Task 3, night.

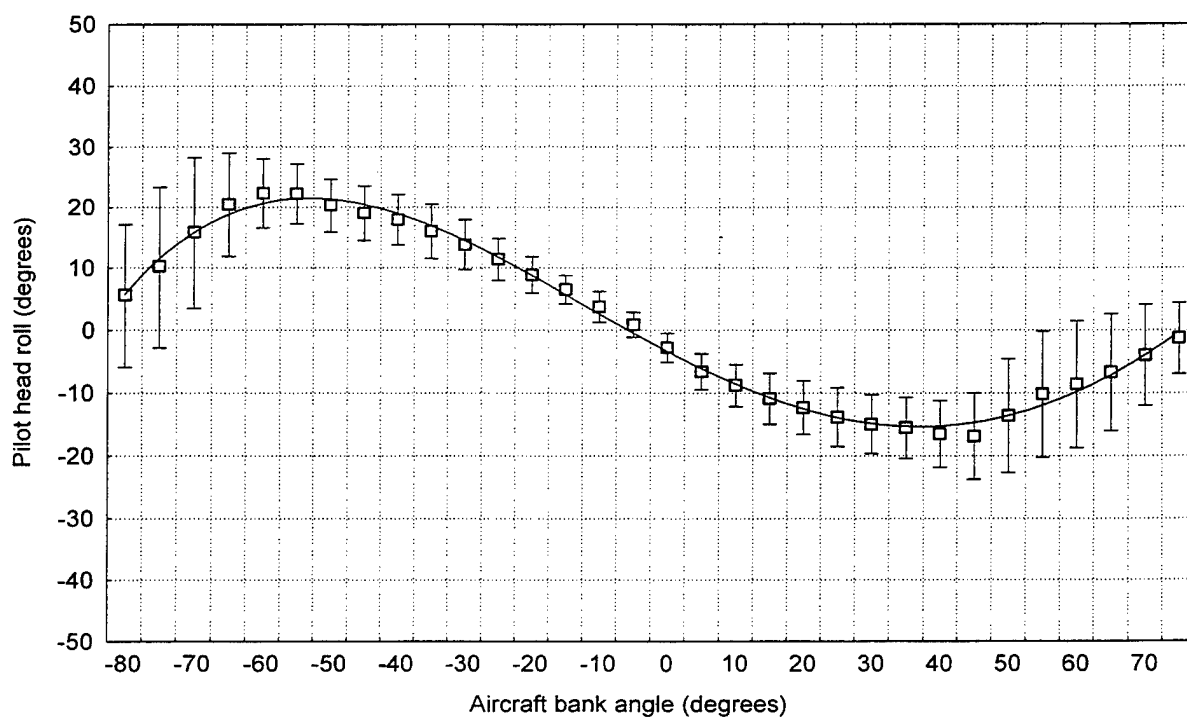


Figure 40. Mean (± 1 SD) head roll as a function of aircraft bank angle. Task 5, night.

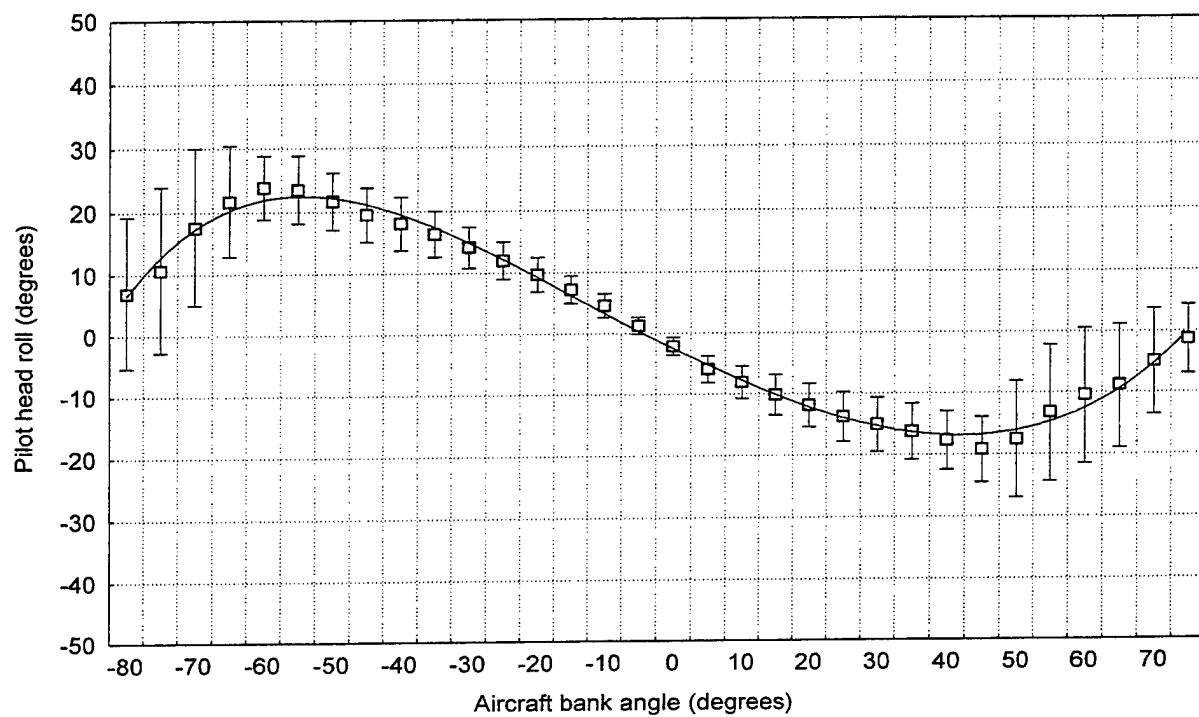


Figure 41. Mean (± 1 SD) head roll as a function of aircraft bank angle. Task 7, night.

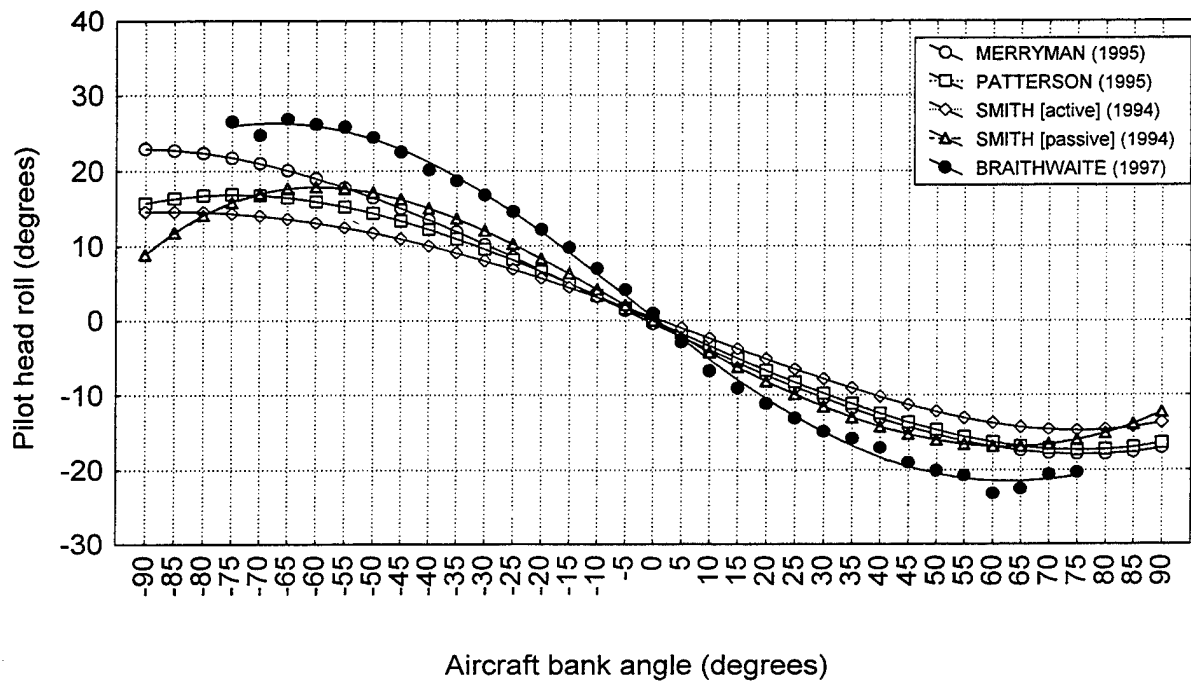


Figure 42. Mean head roll as a function of aircraft bank angle. Comparison with other studies.

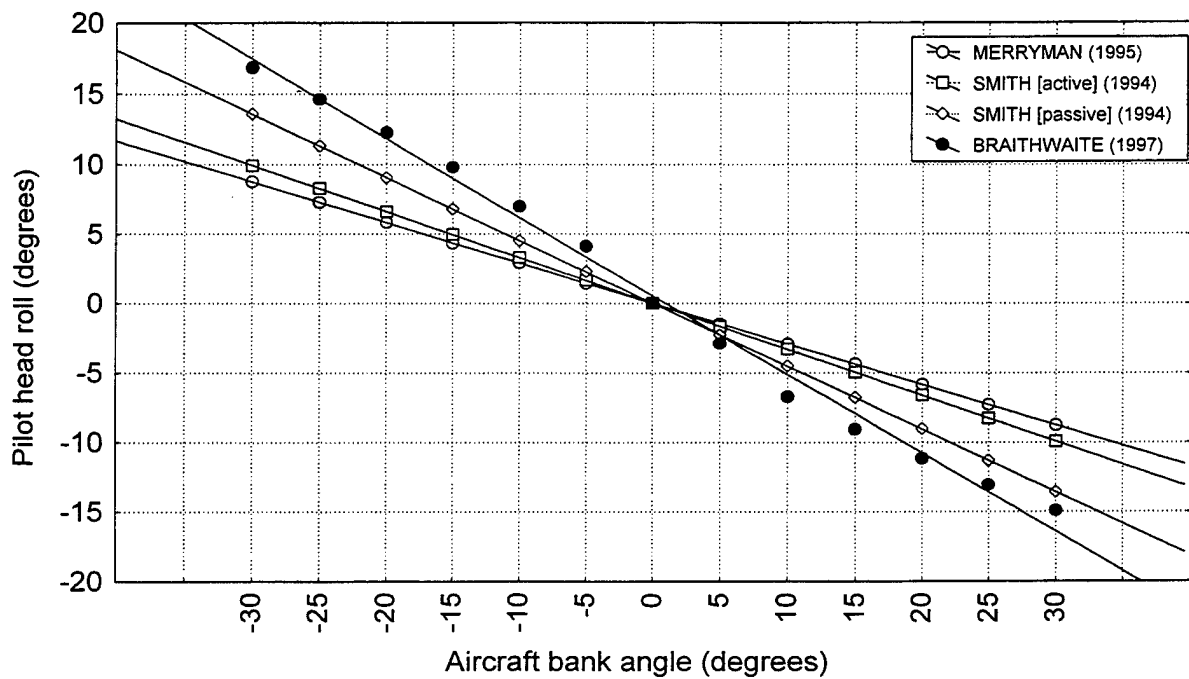


Figure 43. Mean head roll as a function of aircraft bank angle. Comparison of linear segments with other studies.

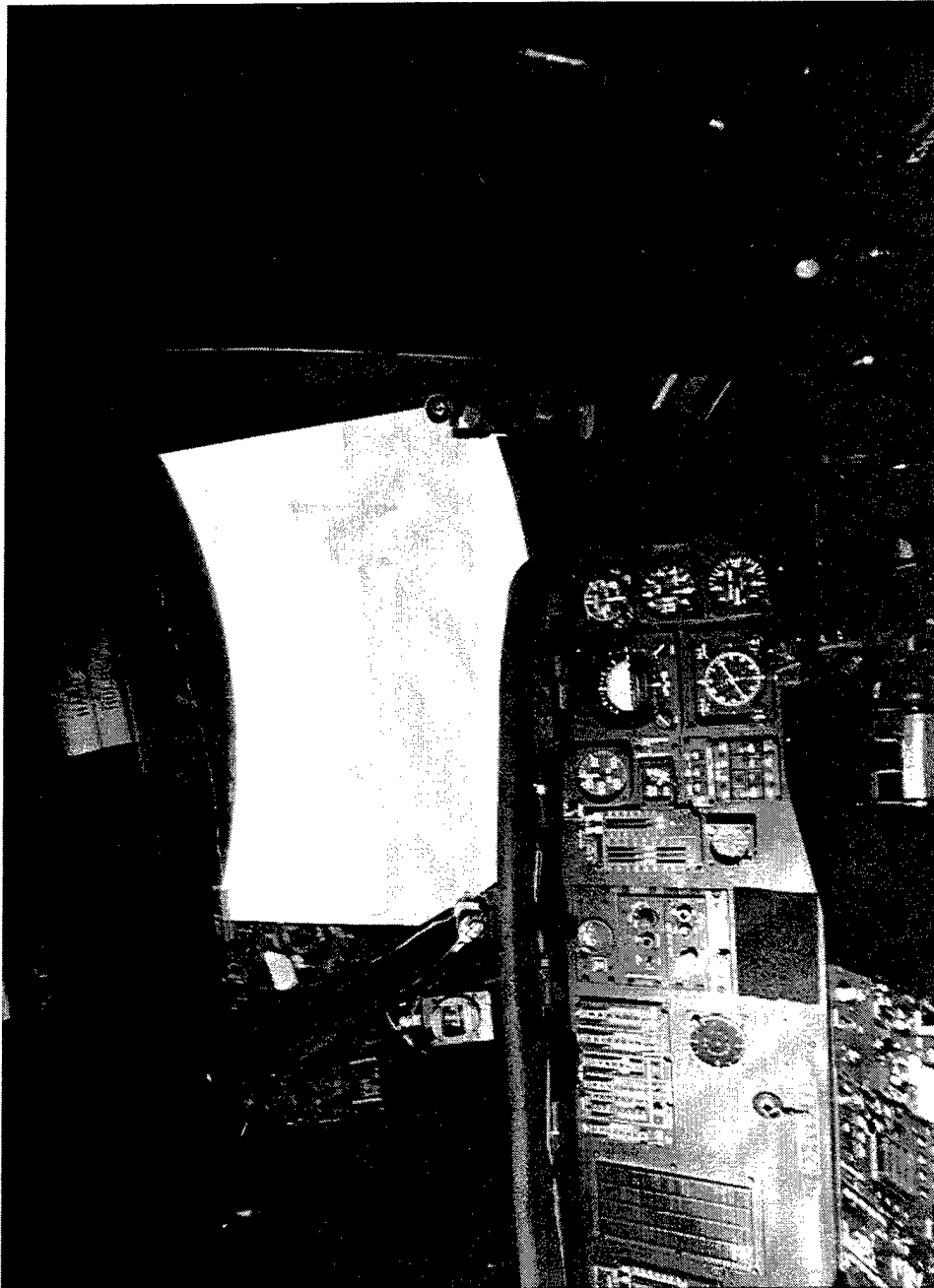


Figure 44. Photograph of UH-60 simulator from the pilot's viewpoint

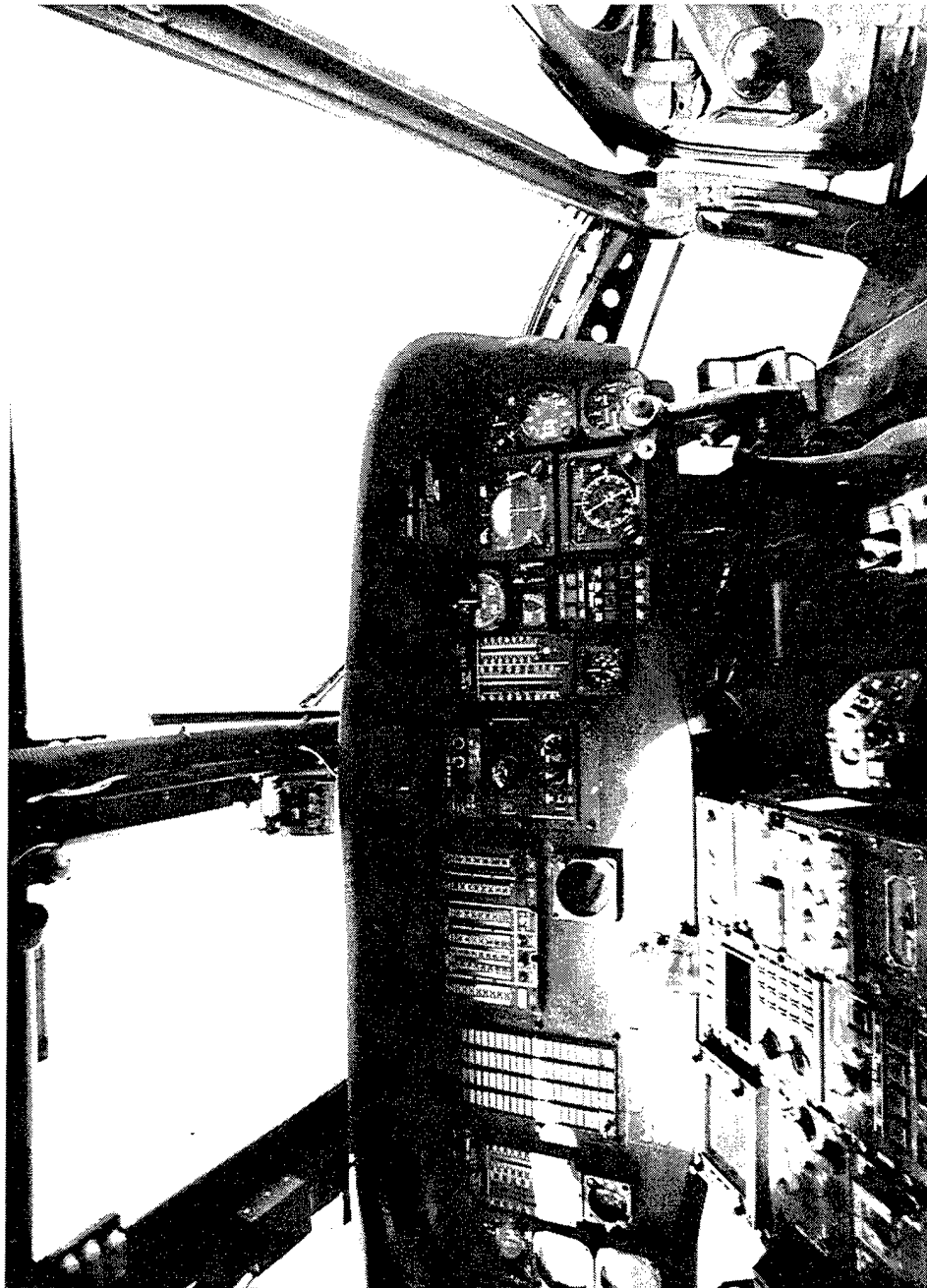


Figure 45. Photograph of UH-60 aircraft from the pilot's viewpoint

References

- Braithwaite, M.G. 1994. An aviation medicine review of Army Air Corps helicopter accidents 1983-1993. Defence Research Agency Center for Human Sciences Report TR94016.
- Braithwaite, M.G., Durnford, S.J., DeRoche, S.L., Alvarez, E.A., Jones, H.D., Higdon, A.A., and Estrada, A. 1997a. Flight simulator evaluation of a novel display to minimize the risks of spatial disorientation. Fort Rucker, AL: U.S. Army Aeromedical Research Laboratory. USAARL Report No. 97-11.
- Braithwaite, M.G., Groh, S.L., and Alvarez, E.A. 1997b. Spatial Disorientation in U.S. Army helicopter accidents: An update of the 1987-92 survey to include 1993-95. Fort Rucker, AL: U.S. Army Aeromedical Research Laboratory. USAARL Report No. 97-27.
- Brandt, T., Dichgans, J., and Koenig, E. 1972. Differential effects of central versus peripheral vision on egocentric and exocentric motion perception. Experimental Brain Research, 16: 476-491.
- Cheung, B., Money, K., Wright, H., and Bateman, W. 1995. Spatial disorientation-implicated accidents in Canadian Forces, 1982-92. Aviat Space Environ Med; 66: 579-85.
- Dehart, R.L. 1985. Fundamental of Aerospace Medicine. 2nd ed. pp 360-369. Philadelphia, PA: Lea and Febiger.
- Durnford, S.J., Crowley, J.S., Rosado, N.R., Harper, J., and DeRoche, S. 1995. Spatial disorientation: A Survey of U.S. Army Helicopter Accidents 1987-92. Fort Rucker, AL: U.S. Army Aeromedical Research Laboratory. USAARL Report No. 95-25.
- Friederici, A.D., Levalt, W.J.M. 1987. Resolving perceptual conflicts: the cognitive mechanism of spatial orientation. Aviat, Space, Environ Med; 58: A164-A169.
- Gillingham, K.K. 1992. Spatial Disorientation problem in the United States Air Force. Journal of Vestibular Research, 2:297-306.
- Gillingham, K.K., Previc, F.H. 1993. Spatial Orientation in Flight. Air Force Material Command, Brooks Air Force Base, Tx. Tech. Report ALTR-1993-0022.
- Gower, D.W., Fowkles, J. 1989. Simulator Sickness in the UH-60 (Black Hawk) flight simulator. Fort Rucker, AL: U.S. Army Aeromedical Research Laboratory. USAARL Report No. 89-25.

Lane, N.E., Kennedy, R.S. 1988. A new method for quantifying simulator sickness questionnaire (SSQ). Essex Corp, Orlando, Florida. Technical Report EOTR 88-7.

McLean, W.E. 1997. Personal communication.

Memorandum. 1996. Memorandum for Commander, U.S. Army Safety Center, dated 18, November (MCMR-UAS-AF) Fort Rucker, AL.

Merryman, R.F.K., Cacioppo, B.S. 1997. The opto-kinetic cervico reflex in pilots of high performance aircraft. Aviat Space Environ Med; 68: 479-487.

Patterson, F.R. 1995. Aviation spatial orientation in relationship to head position and attitude interpretation. Doctor of philosophy dissertation. Wright State University, OH.

Sanders, M.S., McCormick, E.J. 1993. Human factors in engineering and design. 7th edition. New York, NY: McGraw Hill Publishing Company.

Smith, D.R., Cacioppo, B.S., Hinman, G.E. 1997. Aviation spatial orientation in relationship to head position, attitude interpretation, and control. Aviat Space Environ Med; 68: 472-478.

United States Navy. 1986. NATOPS Instrument Flight Manual. Office of the Chief of Naval Operations, Washington D.C. NAVAIR 00-80T112.

Weintraub, D.J., Ensing, M. 1992. Human Factors issues in head-up displays design. CSERIAC, Wright-Patterson AFB, OH.

Woodson, W.E., Tillman, B., Tillman, P. 1992. Human factors design handbook. 2nd rev. New York: McGraw-Hill.

Appendix A.
Head tracker calibration data.

Yaw	Head tracker readings	
	Calibration readings	
	Pre data collection	Post data collection
-45	-44	-43
-30	-29	-29
-20	-19	-19
-10	-9	-9
0	0	0
10	10	9
20	20	18
30	30	28
45	45	43

Pitch	Head tracker readings	
	Calibration readings	
	Pre data collection	Post data collection
-30	-27	-28
-20	-19	-18
-10	-9	-8
0	0	0
10	9	9
20	19	18
30	30	27

Roll	Head tracker readings	
	Calibration readings	
	Pre data collection	Post data collection
-30	-30	-29
-20	-19	-19
-10	-9	-10
0	0	0
10	10	10
20	20	20
30	29	30

Appendix B.
Summary of r-square values.

Table B-1.
Summary of r-square values for day tasks.

Subject	Task 1 DT1	Task 2 DT2	Task 3 DT3	Task 4 DT4	Task 5 DT5	Task 6Y DT6Y	Task 6Z DT6Z
1	0.9774	0.9822	0.9163	0.3369	0.9574	0.9697	0.9250
2	0.9464	0.9752	0.9372	0.9036	0.9407	0.9879	0.8847
3	0.9870	0.9878	0.9324	0.5745	0.9749	0.9749	0.8967
4	0.9849	0.9606	0.9105	0.4615	0.9876	0.9039	0.9824
5	0.9510	0.9856	0.9104	0.5550	0.9077	0.9935	0.7721
6	0.9576	0.9710	0.9248	0.7459	0.9639	0.9440	0.5049
7	0.9787	0.9968	0.9493	0.1211	0.9827	0.9846	0.8127
8	0.8965	0.9400	0.8527	0.8574	0.9234	0.5923	0.8733
9	0.9897	0.9687	0.9566	0.3914	0.9806	0.8974	0.7697
10	0.9457	0.9731	0.9347	0.0023	0.9729	0.9910	0.8044
11	0.9865	0.9910	0.9824	0.9715	0.9728	0.9680	0.8978
12	0.9394	0.9664	0.9743	0.0985	0.9750	0.9946	0.9271
13	0.9422	0.9888	0.8779	0.1848	0.9487	0.9620	0.8446
14	0.9272	0.9722	0.9273	0.1096	0.9861	0.9697	0.9210
15	0.9811	0.9792	0.9679	0.6269	0.9677	0.9737	0.7163
16	0.9917	0.9777	0.9451	0.9634	0.9719	0.9867	0.9008
17	0.9841	0.9814	0.9344	0.1062	0.9859	0.9955	0.8505
18	0.9600	0.9841	0.9633	0.8739	0.9674	0.9682	0.8231
19	0.9822	0.9714	0.9720	0.7983	0.9674	0.9712	0.8180
20	0.9715	0.9686	0.9284	0.2475	0.9432	0.9926	0.8789

shaded cells refer to text remarks in the results section

Table B-2.
Summary of r-square values for night tasks.

Subject	Task 1 NT1	Task 2 NT2	Task 3 NT3	Task 5 NT5
1	0.9698	0.9821	0.9599	0.9747
2	0.9635	0.9525	0.9573	0.9563
3	0.9869	0.9747	0.9380	0.9781
4	0.9928	0.9829	0.9422	0.9834
5	0.8834	0.9861	0.8830	0.9149
6	0.9682	0.9680	0.9627	0.9726
7	0.9906	0.9926	0.9530	0.9511
8	0.8959	0.9260	0.9533	0.9688
9	0.9799	0.9492	0.9499	0.9491
10	0.9794	0.9554	0.9414	0.9794
11	0.9810	0.9675	0.9707	0.9882
12	0.9824	0.9824	0.9826	0.9577
13	0.9501	0.9668	0.9208	0.9627
14	0.9485	0.9661	0.9554	0.9775
15	0.9773	0.9884	0.9807	0.9778
16	0.9748	0.9707	0.9451	0.9681
17	0.9745	0.9722	0.9554	0.9809
18	0.9674	0.9777	0.9624	0.9600
19	0.9844	0.9903	0.9305	0.9682
20	0.9486	0.9816	0.9793	0.9730

Table B-3.
Summary of r-square values from day and night tasks.

Subject	Task 1 Day DT1	Task 2 Day DT2	Task 3 Day DT3	Task 5 Day DT5	Task 7 Day DT7	Task 1 Night NT1	Task 2 Night NT2	Task 3 Night NT3	Task 5 Night NT5	Task 7 Night NT7
1	0.9774	0.9822	0.9163	0.9574	0.9559	0.9698	0.9821	0.9599	0.9747	0.9661
2	0.9464	0.9752	0.9372	0.9407	0.9584	0.9635	0.9525	0.9573	0.9563	0.9574
3	0.9870	0.9878	0.9324	0.9749	0.9697	0.9869	0.9747	0.9380	0.9781	0.9772
4	0.9849	0.9606	0.9105	0.9876	0.9804	0.9928	0.9829	0.9422	0.9834	0.9875
5	0.9510	0.9856	0.9104	0.9077	0.9242	0.8834	0.9861	0.8830	0.9149	0.9470
6	0.9576	0.9710	0.9248	0.9639	0.9769	0.9682	0.9680	0.9627	0.9726	0.9929
7	0.9787	0.9968	0.9493	0.9827	0.9890	0.9906	0.9926	0.9530	0.9511	0.9775
8	0.8965	0.9400	0.8527	0.9234	0.9646	0.8959	0.9260	0.9533	0.9688	0.9689
9	0.9897	0.9687	0.9566	0.9806	0.9771	0.9799	0.9492	0.9499	0.9491	0.9270
10	0.9457	0.9731	0.9347	0.9729	0.9741	0.9794	0.9554	0.9414	0.9794	0.9833
11	0.9865	0.9910	0.9824	0.9728	0.9887	0.9810	0.9675	0.9707	0.9882	0.9866
12	0.9394	0.9664	0.9743	0.9750	0.9691	0.9824	0.9824	0.9826	0.9577	0.9641
13	0.9422	0.9888	0.8779	0.9487	0.9703	0.9501	0.9668	0.9208	0.9627	0.9554
14	0.9272	0.9722	0.9273	0.9861	0.9733	0.9485	0.9661	0.9554	0.9775	0.9694
15	0.9811	0.9792	0.9679	0.9677	0.9757	0.9773	0.9884	0.9807	0.9778	0.9555
16	0.9917	0.9777	0.9451	0.9719	0.9721	0.9748	0.9707	0.9451	0.9681	0.9584
17	0.9841	0.9814	0.9344	0.9859	0.9875	0.9745	0.9722	0.9554	0.9809	0.9900
18	0.9600	0.9841	0.9633	0.9674	0.9814	0.9674	0.9777	0.9624	0.9600	0.9749
19	0.9822	0.9714	0.9720	0.9674	0.9533	0.9844	0.9903	0.9305	0.9682	0.9817
20	0.9715	0.9686	0.9284	0.9432	0.9597	0.9486	0.9816	0.9793	0.9730	0.9884

Table B-4.
Summary of r-square values from motion/nonmotion tasks.

Task	Day/night	Motion On / off	Subject 5	Subject 10	Subject 11	Subject 14
1	Day	On	0.95113	0.94621	0.98662	0.92723
2	Day	On	0.98560	0.97295	0.99106	0.97225
3	Day	On	0.91048	0.93457	0.98241	0.92707
4	Day	On	0.55495	0.00232	0.97149	0.10957
5	Day	On	0.90754	0.97280	0.97284	0.98611
7	Day	On	0.92409	0.97403	0.98871	0.97324
1	Day	Off	0.95045	0.93028	0.99194	0.97184
2	Day	Off	0.98893	0.93185	0.96058	0.97713
3	Day	Off	0.88150	0.95490	0.90625	0.85198
4	Day	Off	0.80887	0.57882	0.96632	0.69914
5	Day	Off	0.96156	0.95936	0.94990	0.96763
7	Day	Off	0.97496	0.95806	0.96501	0.91865
1	Night	On	0.88352	0.97934	0.98116	0.94817
2	Night	On	0.98606	0.95549	0.96741	0.96597
3	Night	On	0.88245	0.94120	0.97092	0.95572
5	Night	On	0.91511	0.97944	0.98812	0.97754
7	Night	On	0.94700	0.98323	0.98666	0.96915
1	Night	Off	0.93664	0.97684	0.96972	0.93366
2	Night	Off	0.97438	0.97609	0.95578	0.94769
3	Night	Off	0.90752	0.92611	0.94202	0.94242
5	Night	Off	0.94043	0.96463	0.93646	0.95711
7	Night	Off	0.93691	0.96053	0.97523	0.92582

shaded cells refer to text remarks in the results section